Cell Reports
Methods

Article

Development of an efficient reproducible cell-cell transmission assay for rapid quantification of SARS-CoV-2 spike interaction with hACE2

Graphical abstract

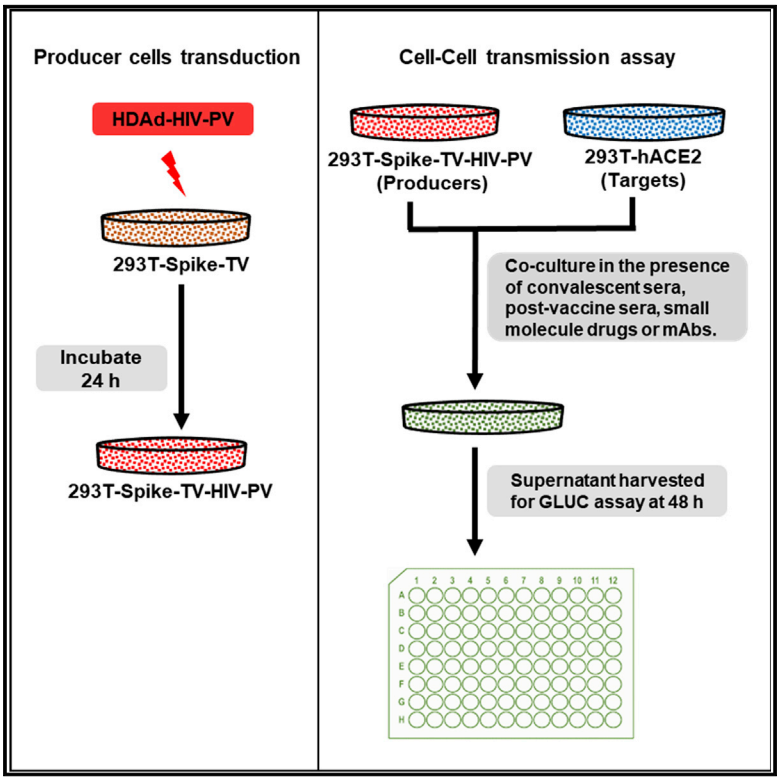

Highlights

- An efficient cell-cell transmission assay for SARS-CoV-2 spike-hACE2 interaction
- Uses two stable cell lines and a single, helper-dependent adenovirus vector
- Reliably tests effects of small-molecule drugs, monoclonal antibodies, and vaccines
- Rapid, reproducible assay, easily modifiable to encode spike variants of concern

Authors

George Ssenyange, Maya Kerfoot, Min Zhao, ..., Charles S. Dela Cruz, Shaili Gupta, Richard E. Sutton

Correspondence

shaili.gupta@yale.edu (S.G.), richard.sutton@yale.edu (R.E.S.)

In brief

Ssenyange et al. describe an efficient, reproducible cell-cell transmission assay for rapid quantification of SARS-CoV-2 spike interaction with hACE2 that can be used to test the effects of convalescent/post-vaccination serum, monoclonal antibodies, and small-molecule drugs. It can be adapted for clinical settings and to test spike variants of concern.

Ssenyange et al., 2022, Cell Reports Methods 2, 100252
July 18, 2022
https://doi.org/10.1016/j.crmeth.2022.100252

CellPress

Cell Reports Methods

CellPress
OPEN ACCESS

Article

Development of an efficient reproducible cell-cell transmission assay for rapid quantification of SARS-CoV-2 spike interaction with hACE2

George Ssenyange,[1] Maya Kerfoot,[1] Min Zhao,[1] Shelli Farhadian,[1] Sidi Chen,[4] Lei Peng,[4] Ping Ren,[4] Charles S. Dela Cruz,[3] Shaili Gupta,[2,5,*] and Richard E. Sutton[1,5,6,*]

[1]Department of Medicine, Section of Infectious Diseases, Yale School of Medicine, New Haven, CT 06510, USA
[2]Department of Medicine, Section of General Internal Medicine, Yale School of Medicine, New Haven, CT 06510, USA
[3]Department of Medicine, Section of Pulmonary and Critical Care Medicine, Yale School of Medicine, New Haven, CT 06510, USA
[4]Department of Genetics, Yale School of Medicine, New Haven, CT 06510, USA
[5]Department of Medicine, Veterans Affairs Healthcare Systems of Connecticut, West Haven, CT 06516, USA
[6]Lead contact
*Correspondence: shaili.gupta@yale.edu (S.G.), richard.sutton@yale.edu (R.E.S.)
https://doi.org/10.1016/j.crmeth.2022.100252

MOTIVATION Reproducible and facile methods of measuring viral replication are indispensable in the development of vaccines and therapeutic medications against SARS-CoV-2. We sought to develop a rapid, time-saving, cell-cell transmission assay that can be used to measure and quantify SARS-CoV-2 virus-cell binding and entry to circumvent the challenges faced by the assays currently used as gold standards for SARS-CoV-2 neutralization studies.

SUMMARY

Efficient quantitative assays for measurement of viral replication and infectivity are indispensable for future endeavors to develop prophylactic or therapeutic antiviral drugs or vaccines against SARS-CoV-2. We developed a SARS-CoV-2 cell-cell transmission assay that provides a rapid and quantitative readout to assess SARS-CoV-2 spike hACE2 interaction in the absence of pseudotyped particles or live virus. We established two well-behaved stable cell lines, which demonstrated a remarkable correlation with standard cell-free viral pseudotyping for inhibition by convalescent sera, small-molecule drugs, and murine anti-spike monoclonal antibodies. The assay is rapid, reliable, and highly reproducible, without a requirement for any specialized research reagents or laboratory equipment and should be easy to adapt for use in most investigative and clinical settings. It can be effectively used or modified for high-throughput screening for compounds and biologics that interfere with virus-cell binding and entry to complement other neutralization assays currently in use.

INTRODUCTION

Coronavirus disease 2019 (COVID-19), due to the novel severe acute respiratory syndrome coronavirus 2 (SARS-CoV-2), has become an ongoing, persistent global public health challenge since its emergence in December 2019 (Vogel, 2020), with over 260 million confirmed cases worldwide and close to 5.2 million COVID-19-related deaths as of November 30, 2021 (https://coronavirus.jhu.edu/), despite the wide availability of multiple fully approved safe and efficacious vaccines.

SARS-CoV-2 is a betacoronavirus, belonging to the genus *Coronavirus*, in the family *Coronaviridae*. It is an enveloped, non-segmented, positive-sense single-stranded RNA virus (Li et al., 2020a; Chan et al., 2020). It has a genome nearly 30 kb in length, including many open reading frames (ORFs), which express at least 27 proteins (Chan et al., 2020; Wu et al., 2020a). The surface spike glycoprotein (S) plays a key role in viral entry into target host cells (Wrapp et al., 2020; Bosch et al., 2003). The receptor-binding subunit S1 attaches to the host cell via the cellular receptor human angiotensin-converting enzyme 2 (hACE2), triggering proteolytic activation of S and subsequent conformational changes of the S2 subunit, which facilitates the fusion of viral and cellular membranes (Huang et al., 2020; Li et al., 2003, 2020b).

Currently, the development of numerous prophylactic and therapeutic strategies is in progress to mitigate this global public health crisis (Klasse and Moore, 2020; Lythgoe and Middleton, 2020; Sarma et al., 2020; Wang et al., 2020a), including the

use of small-molecule drugs (Riva et al., 2020); biologics, including interferon (Shalhoub, 2020); convalescent sera (Bloch et al., 2020; Casadevall and Pirofski, 2020); monoclonal antibodies (Zost et al., 2020; Zhou and Zhao, 2020; Wu et al., 2020b; Ho et al., 2020; Pinto et al., 2020; Liu et al., 2020; Ju et al., 2020; Jiang et al., 2020; Cao et al., 2020b); oligonucleotides (Rehman and Tabish, 2020); peptides (VanPatten et al., 2020); and vaccines (Yu et al., 2020; Graham, 2020; Wang and Zhang, 2020). Remdesivir remains the only US Food and Drug Administration (FDA)-approved antiviral drug for use in adults and pediatric patients for treatment of COVID-19 requiring hospitalization (https://www.fda.gov/drugs/news-events-human-drugs/fdas-approval-veklury-remdesivir-treatment-covid-19-science-safety-and-effectiveness). Three vaccines have emergency use authorization (EUA) from the FDA or are fully approved (https://www.fda.gov/emergency-preparedness-and-response/coronavirus-disease-2019-covid-19/covid-19-vaccines), and four vaccines have been formally approved by the European Medicines Agency (EMA) (https://www.ema.europa.eu/en/human-regulatory/overview/public-health-threats/coronavirus-disease-covid-19/treatments-vaccines/covid-19-vaccines). A few SARS-CoV-2-targeting monoclonal antibodies (mAbs) have also been approved through an EUA for use in COVID-19 patients meeting eligibility criteria (https://www.fda.gov/drugs/emergency-preparedness-drugs/coronavirus-covid-19-drugs). No other specific antiviral drug against SARS-CoV-2, however, has been formally approved by the FDA or EMA.

Quantitative assays for the measurement of viral replication and infectivity are indispensable for future endeavors to develop prophylactic or therapeutic antiviral drugs or vaccines against SARS-CoV-2. The current gold standards for SARS-CoV-2 neutralization include pseudotyping using S and a suitable virus core encoding a reporter (Jiang et al., 2020; Schmidt et al., 2020; Ou et al., 2020; Zhao et al., 2021; Crawford et al., 2020) or inhibition of live virus replication *in vitro* or in animal models (Zhao et al., 2021; Johansen et al., 2020; Bao et al., 2020). Although it has been previously reported that inhibition of replication-competent virus or pseudotyped particles correlates well with protection from SARS-CoV-2 virus challenge in pre-clinical models of infection (Yu et al., 2020; Chandrashekar et al., 2020; Mercado et al., 2020), these assays require high-level biocontainment and continued production, testing, and cryostorage of virus vector supernatants, which may be variable in quality and differ remarkably from lab to lab. These assays are typically very time consuming, requiring several days to produce and concentrate the virus to achieve a suitably high titer, with assay readout on susceptible cells after a few days (Quinonez and Sutton, 2002); live coronavirus requires a BSL3 laboratory and readout by plaque or similar quantitative assay several days after cell or animal infection, performed *in vitro* or *in vivo*, respectively.

To circumvent some of these issues, we developed a cell-cell transmission-based assay that utilizes producer cells expressing S, an HIV packaging vector, and an HIV-based transfer vector, which, when co-cultured together with hACE2-expressing target cells, provide a rapid and quantitative readout to assess S-hACE2 interaction in the absence of producing or using pseudotyped particles or live virus. The assay is very rapid, reliable, and highly reproducible; it is easy to implement in most laboratories without need for special reagents or equipment, compared with other assays that rely upon virus production and testing. It can be effectively used or modified for high-throughput screening for compounds and biologics that interfere with virus-cell binding and entry to complement other neutralization assays that are currently in use.

RESULTS

Development of a quantitative cell-cell transmission assay for SARS-CoV-2 in transiently transfected cells

Viruses can spread via either a cell-free or a cell-associated route, the latter involving direct cell-cell contact (Mothes et al., 2010). Cell-cell transmission can occur via a virologic synapse and, at least in the case of HIV, is typically much more efficient than cell-free infection (Sattentau, 2008; Agosto et al., 2015; Chen et al., 2007; Jolly et al., 2004; Jolly and Sattentau, 2004; Martin et al., 2010; Zhong et al., 2013a, 2013b; Abela et al., 2012). Like other coronaviruses, the S protein mediates cell-surface receptor recognition, cell attachment, and fusion during SARS-CoV-2 virus infection of susceptible cells expressing hACE2, its cognate receptor (Li et al., 2003; Ou et al., 2020; Hoffmann et al., 2020; Belouzard et al., 2012; Shang et al., 2020). To measure cell-cell transmission of SARS CoV-2, we employed a system developed by the late David Derse (Mazurov et al., 2010b). We generated target cells expressing hACE2, the cognate receptor for SARS-CoV-2, and producer cells that were transiently transfected with plasmid DNAs to introduce S, along with all requisite *trans*-acting factors for HIV core production (HIV packaging vector or HIV-PV) and an HIV-based transfer vector (HIV-TV), as described under STAR Methods and illustrated in Figure 1A.

To validate the cell-cell transmission assay, we initially tested whether the assay is dependent on the expression of S and HIV-PV by producer cells and the expression of hACE2 by target cells. HIV-TV was transfected into 293T cells in the presence or absence of HIV-PV and either empty plasmid, plasmid encoding Wuhan S, or a vesicular stomatitis virus (VSV) G expression plasmid. After 48 h these cells were mixed with 293T or 293T-hACE2 cells, and 48 h later the culture supernatant was assessed for relative light unit (RLU) activity. As shown in Figure 1C, RLU values were close to background (<10) without any glycoprotein added; in the presence of S, RLUs increased ~4,000-fold. Compared with target cells without hACE2, RLUs increased ~10-fold in the presence of hACE2 (Figure 1D). In the absence of HIV-PV, RLU activity was <10, essentially a background value (Figure 1C). As anticipated, cell-cell transmission in the presence of VSV G was not dependent on hACE2, since its cognate receptor is ubiquitous in mammalian eukaryotic cells (Figure 1F).

Convalescent sera from COVID-19+ patients and post-vaccination sera inhibit cell-cell transmission in transiently transfected cells

We next investigated the effects of convalescent sera from COVID-19+ patients and post-vaccination sera on cell-cell transmission, initially using transiently transfected cells. Convalescent sera from 11 COVID-19+ patients and sera from 11 subjects at 1 month post vaccination were selected at random for testing. Demographic and relevant clinical information of the subjects

CellPress
OPEN ACCESS

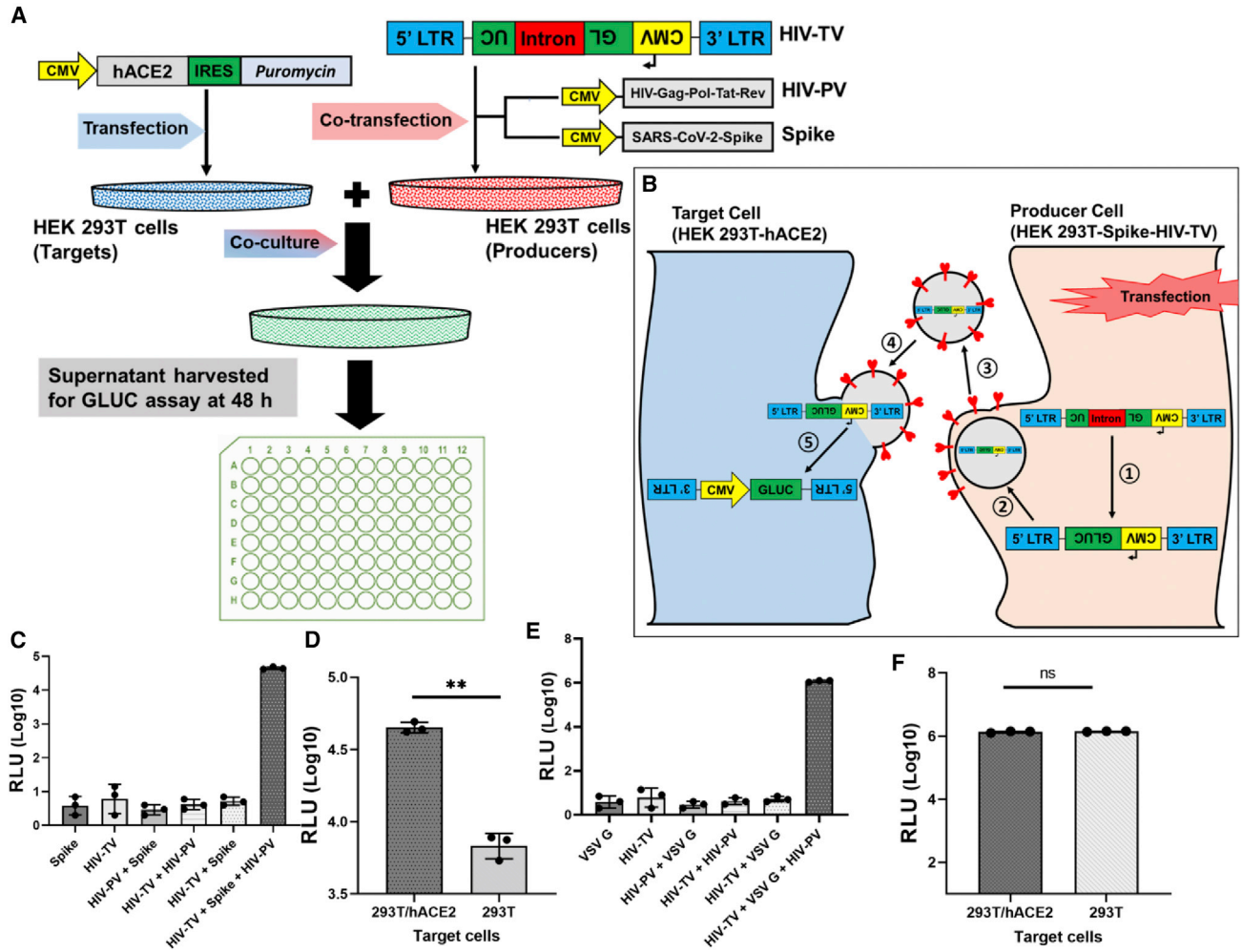

Figure 1. Cell-cell transmission assay is dependent upon the expression of hACE2 in target cells and the HIV packaging vector (HIV-PV), HIV transfer vector (HIV-TV), and viral glycoprotein in producer cells

(A) Schematic illustration of cell-cell transmission assay experimental design.

(B) Schematic illustration of cell-cell transmission at the cellular level, showing how HIV-TV (with a backward or reverse luciferase gene) is activated in the target cells. The *Gaussia* luciferase gene has an intron that is spliced out in the producer cell following transfection (1) and packaged into pseudoparticles (2), which are then released into the culture medium (3). S-pseudotyped particles infect adjacent 293T-hACE2 target cells (4). In the target cell, the vector RNA (now spliced) is reverse transcribed and integrated into the target cell genome, activating the CMV-driven *Gaussia* luciferase gene (5). Note that in the cytosol of the producer cell the vector is RNA, which is also true for released pseudoparticles; only in the target cell is the vector RNA converted to dsDNA and then integrated into the target cell genome.

(C–F) pHIV-TV was transfected into 293T cells in the presence or absence of HIV-PV and either empty plasmid, plasmid encoding spike, or VSV G. After 48 h these cells were mixed with 293T or 293T-hACE2 targets, and 48 h later the culture supernatant was assessed for *Gaussia* luciferase activity. The paired t tests for two-group comparison were analyzed using GraphPad Prism software. ns, not significant; **$p < 0.01$.

is shown in Tables S1 and S2 for convalescent and post-vaccination sera, respectively. Four-fold serial dilutions of convalescent and post-vaccination sera were pre-incubated with S-expressing producer cells for 1 h, and then hACE2-expressing target cells were added, performed in triplicate. RLU was measured after 48 h, and IC_{50} values were calculated. Apart from two sera (one convalescent, Figure 2E, and one post vaccination, Figure 3E), we observed that convalescent (Figures 2A–2D) and post-vaccination (Figures 3A–3D) sera inhibited cell-cell transmission of S in the transient system, with a strong positive correlation with the results we observed with S pseudotyping using the same sera (Figures 2H and 3H for convalescent and post-vaccination sera, respectively). No inhibition by convalescent or post-vaccination sera was observed with cell-cell transmission using VSV G, as anticipated (Figures 2F and 3F).

Studies with LCB1 peptide and small-molecule drugs in the transient system

We then investigated the effect of LCB1 (56-mer peptide) and small-molecule drugs, including apilimod, cobicistat, clofazimine, niclosamide, 25-hydroxycholesterol, 27-hydroxycholesterol, and mycophenolate (MPA), all previously reported to be inhibitory to

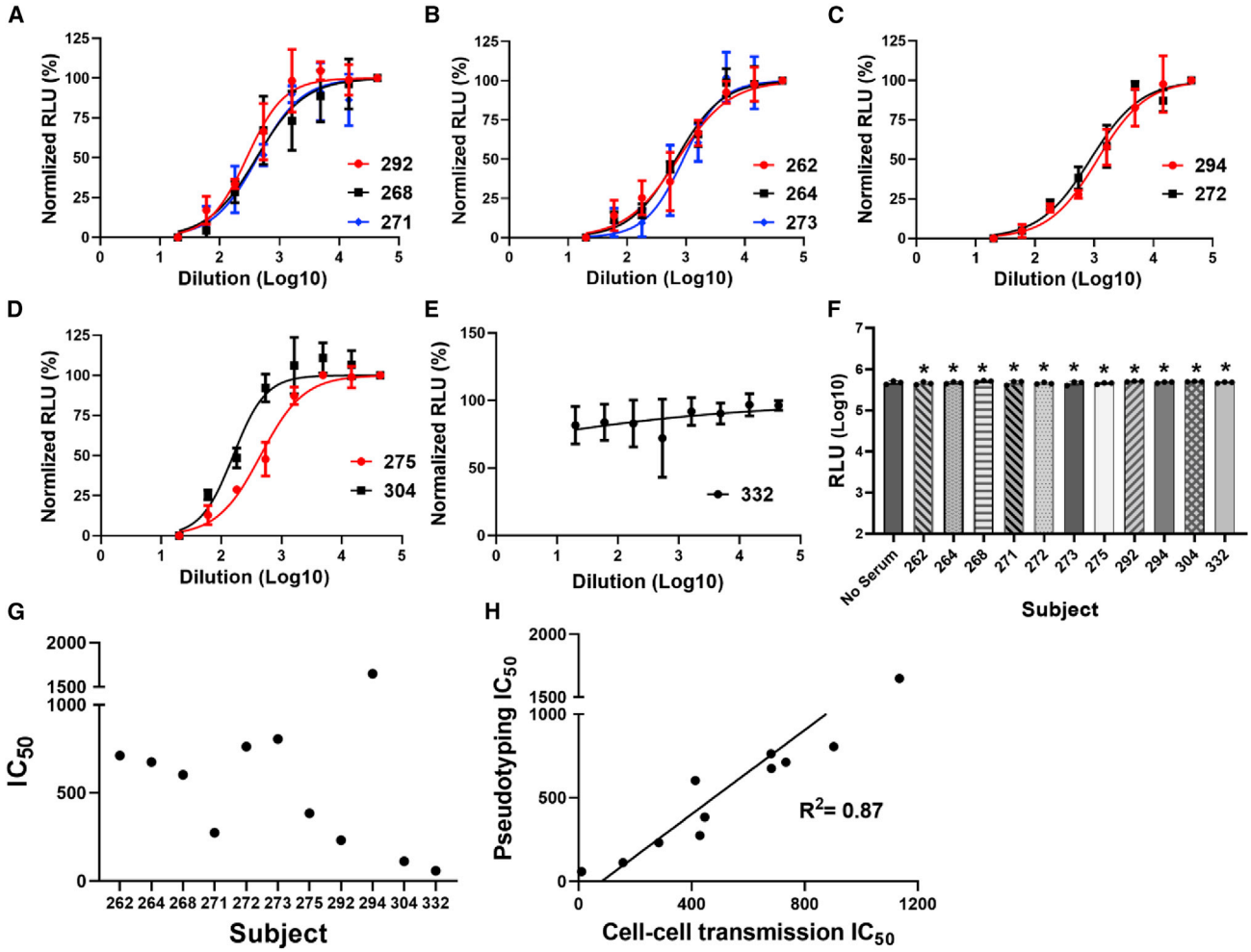

Figure 2. COVID-19+ convalescent sera inhibit spike-mediated cell-cell transmission in the transient system

(A–D) Four-fold serial dilutions of convalescent sera were pre-incubated with spike-expressing producer cells for 1 h, and then hACE2-expressing target 293T cells were added, performed in triplicate. RLU was measured after 48 h, and IC_{50} values were calculated.

(E) One serum sample showed no inhibitory effect.

(F) No inhibition of VSV G pseudotyped virus was observed at the lowest serum dilution tested (1:20). *Not significant compared with no serum control.

(G) IC_{50} values calculated for S pseudotyping using same sera, performed as shown in Figure S1.

(H) Correlation between IC_{50} values for cell-cell transmission and pseudotyping assay for convalescent sera. See also Figures S1 and S4. The paired t tests for two-group comparison were analyzed using GraphPad Prism software.

SARS-CoV-2 infection (Prabhakara et al., 2021; Xie et al., 2020; Yuan et al., 2021; Wang et al., 2020b), on cell-cell transmission of S in the transient system as described under STAR Methods. LCB1 has been reported to efficiently neutralize pseudotyped SARS-CoV-2 virus entry (Cao et al., 2020a). When we tested its ability to inhibit cell-cell transmission of S, the IC_{50} was 0.72 nM (Figure 4A), which is essentially the same as the IC_{50} value for pseudotyping (0.85 nM, Figure 6B). Among the small-molecule drugs, niclosamide was inhibitory of cell-cell transmission of S (IC_{50} of 91 nM; Figure 4B), whereas 25-hydroxycholesterol and 27-hydroxycholesterol were stimulatory, enhancing cell-cell transmission of S with EC_{50} of 23.6 and 8 μM (Figures 4C–4H), respectively. We observed no obvious inhibitory or stimulatory effect of either 25-hydroxycholesterol or 27-hydroxycholesterol on cell-cell transmission when VSV G instead of S was employed as the viral glycoprotein (Figures S3E and S3F, respectively). We observed no obvious inhibitory effect on S cell-cell transmission when using MPA, cobicistat, clofazimine, or apilimod, with each of them having IC_{50} > 10 μM (Figures 4D–4G).

Establishment of stable cell lines to quantify SARS-CoV-2 cell-cell transmission

The results described above demonstrate quantitation of S-mediated cell-cell transmission in transiently transfected 293T cells. Transient transfection of cells is associated with many drawbacks—it is relatively complicated, unreliable, occasionally irreproducible, and not amenable to high-throughput use. We thus sought to develop and establish stable cell lines that can be used to quantify S cell-cell transmission rapidly and reliably with highly reproducible results. We generated a

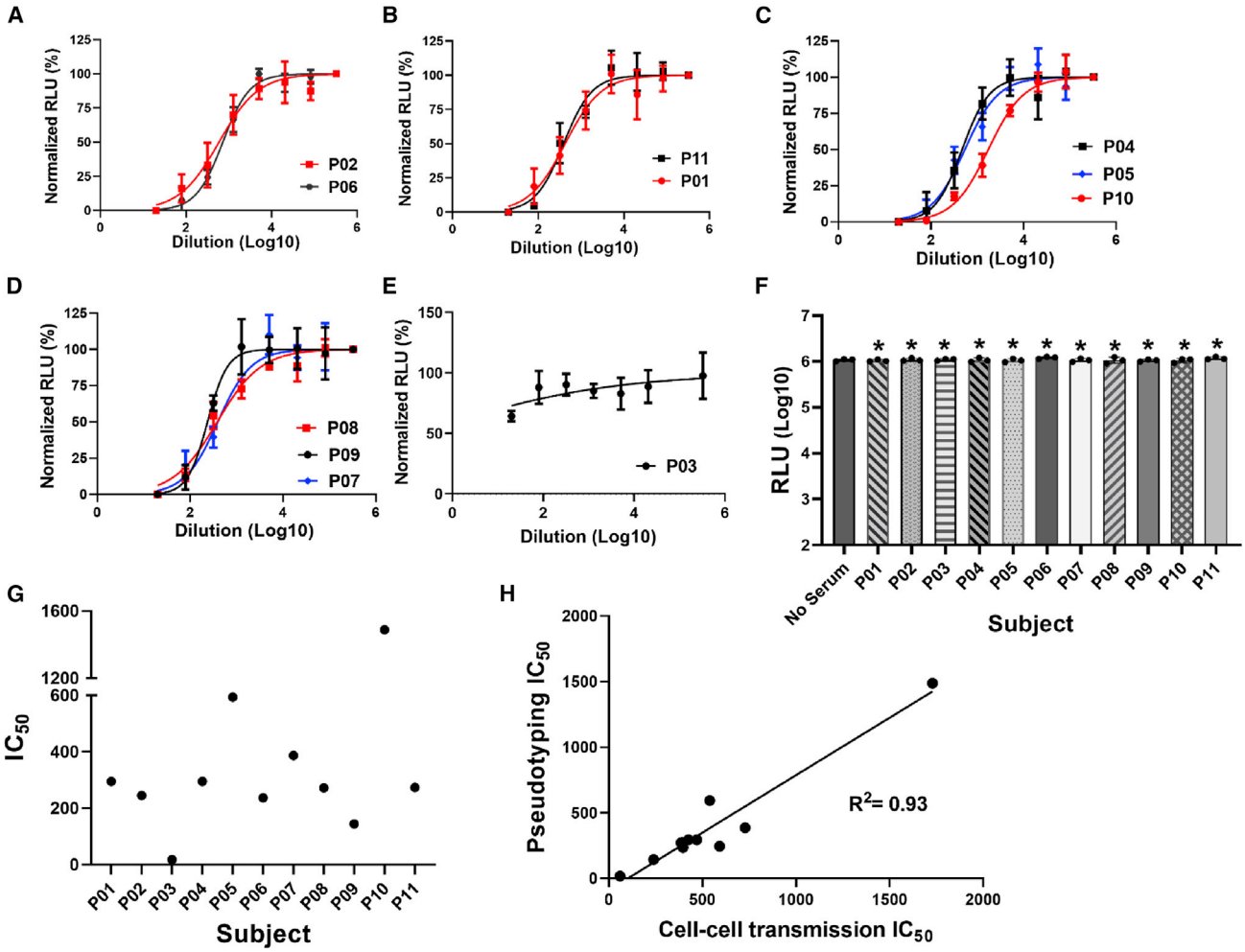

Figure 3. Post-vaccination sera inhibit spike-mediated cell-cell transmission in the transient system

(A–D) Four-fold serial dilutions of post-vaccination sera were pre-incubated with spike-expressing producer cells for 1 h, and then hACE2-expressing target cells were added, performed in triplicate. RLU was measured after 48 h, and IC_{50} values were calculated.

(E) One serum sample showed no inhibitory effect.

(F) No inhibition of VSV G pseudotyped virus was observed at the lowest serum dilution tested (1:20). *Not significant compared with no serum control.

(G) IC_{50} values calculated for S pseudotyping using same sera, performed as in Figure S1.

(H) Correlation between IC_{50} values for the cell-cell transmission and pseudotyping assay for post-vaccination sera. See also Figures S1 and S4. The paired t tests for two-group comparison were analyzed using GraphPad Prism software.

target cell line stably expressing hACE2 (293T-hACE2) and a producer cell line stably expressing Wuhan S and the HIV-TV, in-GLUC (cell line termed 293T-Spike-TV), as described under STAR Methods. Expression of S and hACE2 in these stable cell lines was confirmed by immunoblotting using an anti-FLAG antibody and anti-hACE2 antibody, as shown in Figures S5C and S5D, respectively. Stable expression of HIV-TV was confirmed by nested PCR to show the presence of 3′ long terminal repeat (LTR) sequences (a part of the transfer vector expression cassette, with an expected PCR product of 1.5 kb) using genomic DNA extracted from the stable producer cell line, 293T-Spike-TV (Figure S5E). Despite repeated efforts, we were unable to make a producer cell line stably expressing functional HIV-PV. To circumvent this problem, we utilized a previously described helper-dependent adenovirus (HDAd) vector (Hu et al., 2015) to transiently introduce HIV-PV, as described under STAR Methods. HDAd vectors have shown remarkable consistency and efficiency in the transduction of 293T cells compared with plasmid transfection, with higher levels of HIV structural and enzymatic protein expression (Hu et al., 2015). Expression of HIV Gag by the HDAd-transduced producer cells was confirmed by immunoblot (Figure S5A). This HDAd also encodes the LacZ gene, which serves as a reporter. We transduced 293T-Spike-TV cells with increasing amounts of HDAd-HIV-PV and fixed and stained cells for LacZ expression at 48 h. As the MOI increased, the percentage of blue cells also rose, such that essentially all the cells were transduced at high MOI (Figures S6A and S6B). We titrated the HDAd-HIV-PV to use optimal amounts that resulted in high transduction efficiency with minimal to no cytopathic effect on both the producer and

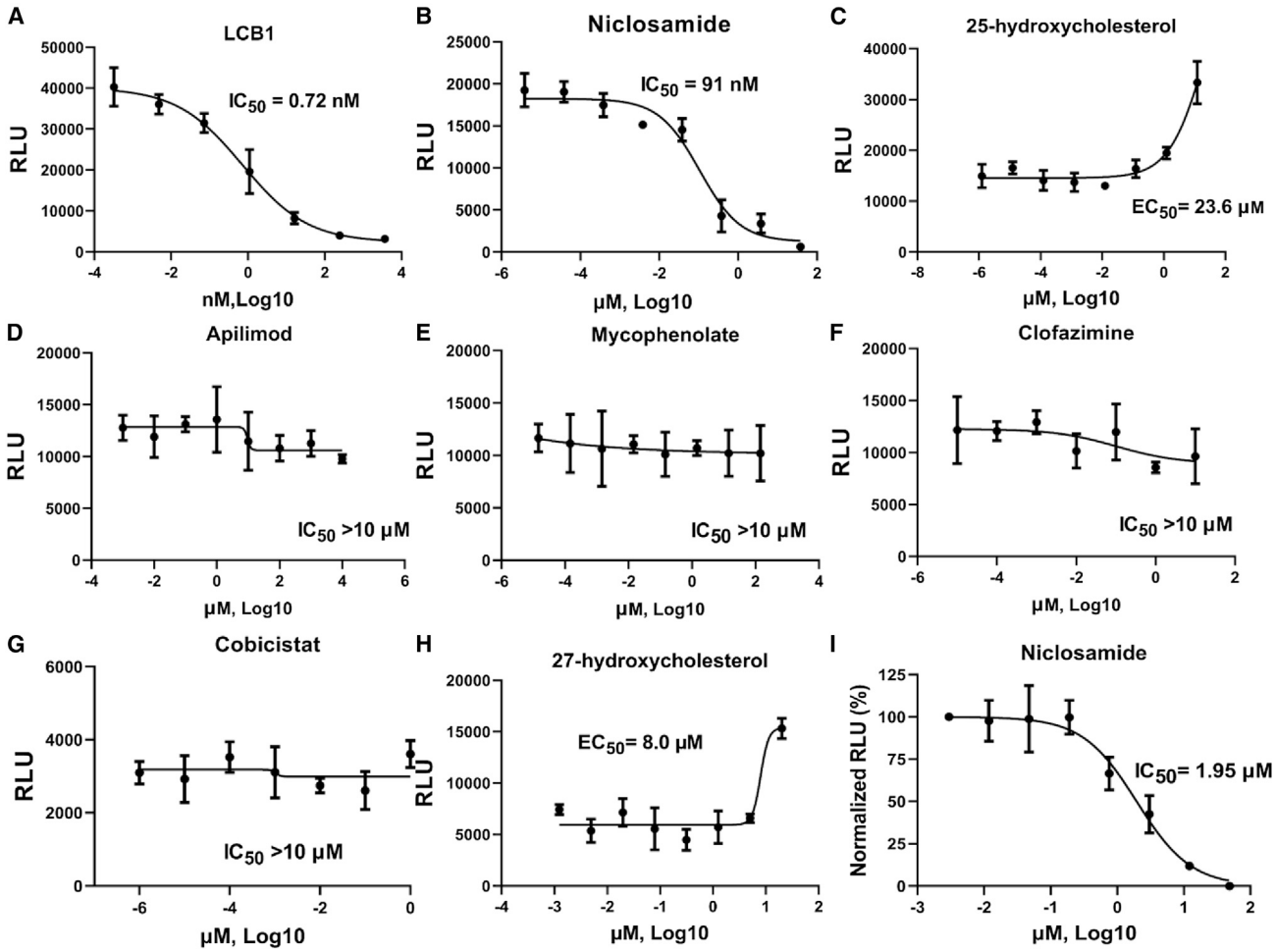

Figure 4. Effect of peptide and small-molecule drugs in the transient system

(A–I) Ten-fold serial dilutions of LCB1 and other small-molecule drugs were pre-incubated with producer cells in parallel for 1 h, and then hACE2-expressing target cells were added, performed in triplicate. LCB1 (A), niclosamide (B), 25-hydroxycholesterol (C), apilimod (D), mycophenolate (E), clofazimine (F), cobicistat (G), and 27-hydroxycholesterol (H) are shown. Niclosamide inhibited cell fusion. Serial dilutions of niclosamide were incubated with TZMbl-Spike producer cells for 1 h. Target cells (HOS-3734) were then added, and RLU was measured the following day (I). See also Figure S4.

the target stable cell lines. When increasing MOI of the HDAd-HIV-PV was employed, the RLU values following co-culture using the stable producer and target cell lines were ~5-fold less compared with the transient system, but still ~10,000-fold above background, with values directly correlated to the amount of HDAd-HIV-PV used for transduction (Figure S6C).

Additional characterization and validation of the stable cell line system

To further characterize and validate the stable cell lines, we tested the effects of LCB1, post-vaccination sera, and small-molecule drugs, including cobicistat, niclosamide, 25-hydroxycholesterol, and 27-hydroxycholesterol, on cell-cell transmission, in comparison with pseudotyping. We tested 11 samples of post-vaccination sera from the same subjects used in the transient system. Demographic and relevant clinical information of the subjects is shown in Table S2. With a single exception, all tested sera inhibited cell-cell transmission at varying titers (Figures 5A–5C). Apart from outlier P03 (Figure 5D), IC_{50} titers for the cell-cell transmission assay varied between 63.8 and 1,560 (Figure 5F). Sera from the same subjects were also tested in the pseudotyping assay (Figure 5E). Although the cell-cell transmission IC_{50} titers were generally higher compared with those of pseudotyping, there was a strong positive correlation between cell-cell transmission and pseudotyping results (Figure 5G), with an R^2 value of 0.94. This is added proof that the cell-cell transmission assay is indeed measuring S-hACE2 interaction and virus infectivity. Unsurprisingly, the post-vaccination IC_{50} titers for the transient and stable cell-cell transmission systems were highly correlated, with an R^2 value of 0.85 (Figure 5H).

Niclosamide was inhibitory in the stable cell-cell transmission assay, with an IC_{50} value of 0.10 µM, ~10-fold lower than that of the pseudotyping (0.96 µM; Figure 6) and ~20-fold lower than that of the cell fusion assay (1.95 µM; Figure 4I). 25-Hydroxycholesterol and 27-hydroxycholesterol were both stimulatory. 25-Hydroxycholesterol enhanced cell-cell

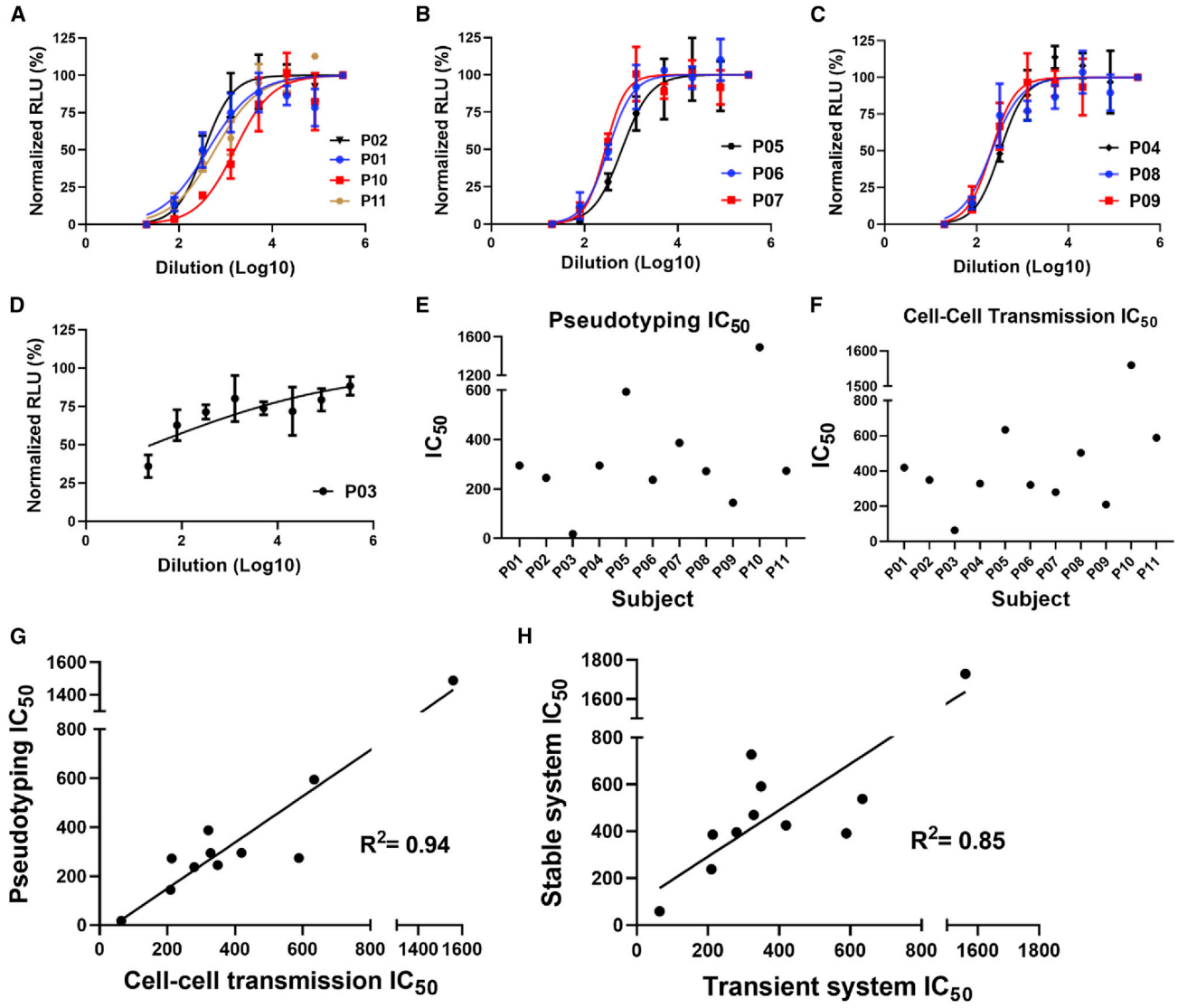

Figure 5. Post-vaccination sera inhibit cell-cell transmission of spike in the stable system

(A–C) Four-fold serial dilutions of post-vaccination sera were pre-incubated with spike-expressing producer cells for 1 h, and then hACE2-expressing target cells were added, performed in triplicate. RLU was measured after 48 h, and IC_{50} values calculated.

(D) One serum sample showed no inhibitory effect.

(E and F) IC_{50} values were calculated for pseudotyping (E) and cell-cell transmission (F), using the same sera.

(G) Correlation between IC_{50} values for cell-cell transmission and pseudotyping assay for post-vaccination sera in the stable system.

(H) Correlation of IC_{50} values for post-vaccination sera in the cell-cell transmission assay between the transient and the stable system. See also Figures S5 and S6.

transmission ~2-fold, with an EC_{50} value of 1.24 μM, whereas 27-hydroxycholesteol had an EC_{50} value of 5.17 μM, enhancing cell-cell transmission ~1.5-fold. This was in contrast to what we observed with S pseudotyping, in which 25-hydroxycholesterol was inhibitory, with an IC_{50} value of 0.45 μM, and 27-hydroxycholesterol had no obvious inhibitory or stimulatory effect on S pseudotyping (Figure 6).

LCB1 peptide was inhibitory, with an IC_{50} of 0.68 nM, which is ~1.3-fold less than that of pseudotyping at 0.85 nM. Moreover, a time-of-addition experiment demonstrated that LCB1 efficiently inhibits cell-cell transmission at −1 and 0 h (with IC_{50} values of 0.68 and 1.37 nM, respectively) before target-producer cell co-culture. The inhibitory effect was reduced when LCB1 was added 1 h after co-culture (IC_{50} of 2.25 nM), and no effect was observed with addition after 2 h, as shown in Figure S2F. A similar trend was observed when we compared LCB1 time-of-addition results with pseudotyping (Figure S2E).

Studies with tetherin and murine anti-spike monoclonal antibodies

Tetherin is an interferon-induced membrane-associated host protein whose expression is known to block the release of

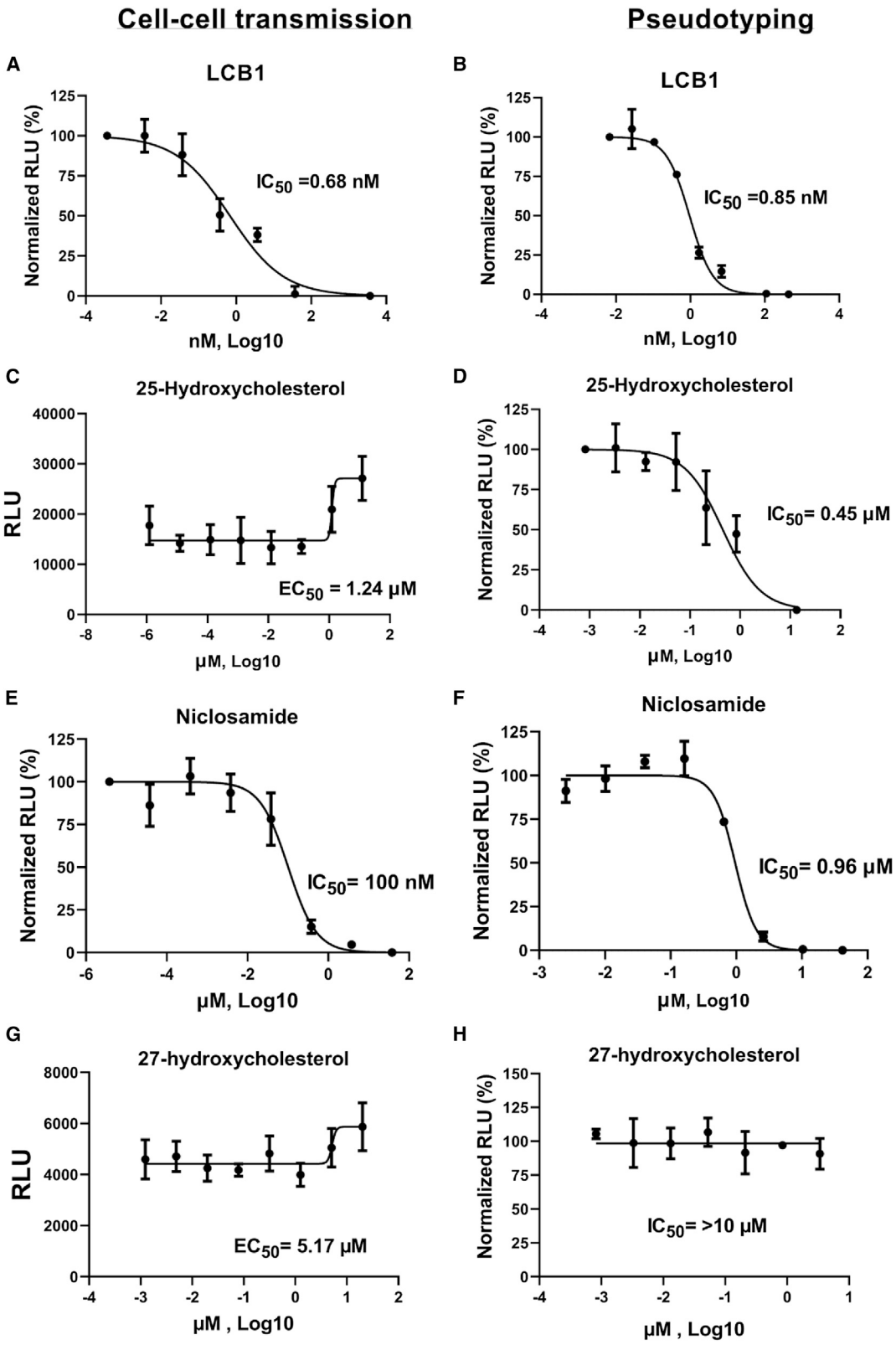

(legend on next page)

HIV-1 and other enveloped viral particles (Perez-Caballero et al., 2009). We tested the effect of increasing amounts of tetherin on cell-cell transmission of SARS-CoV-2 S and how it compared with cell-free S pseudotyping. Producer cells were transiently transfected with increasing amounts of a cytomegalovirus (CMV)-driven plasmid encoding tetherin in a 12-well format for cell-cell transmission and 10-cm plates for pseudotyping, with results normalized to the amount of DNA transfected per surface area (ng/cm^2). We observed an inhibitory effect of increasing amounts of tetherin on both S cell-cell transmission and pseudotyping. However, a more profound effect was seen on S pseudotyping, with a 10-fold decrement in RLU values at the highest amount of tetherin plasmid transfected (48 ng/cm^2; Figure S3B), whereas cell-cell transmission RLU values were reduced only ~2-fold at an even higher tetherin plasmid amount (normalized for plate surface area at 72 ng/cm^2; Figure S3A). A similar trend of effect with tetherin was observed when VSV G instead of S was employed as the viral glycoprotein (Figures S3C and S3D).

We also tested two anti-S murine monoclonal antibodies (clones 2 and 6, both of which bound the receptor-binding domain [RBD]), produced by co-author S.C. Four-fold serial dilutions of each monoclonal antibody were pre-incubated with S-expressing producer cells for 1 h, and then hACE2-expressing target cells were added, performed in triplicate. RLU was measured after 48 h, and IC_{50} values were calculated. Both clone 2 and 6 antibodies had good activity, inhibiting cell-cell transmission with IC_{50} values of 0.53 and 0.14 μg/mL, respectively. Clone 6 was consistently more inhibitory by several fold, compared with clone 2. Results in the transient cell-cell transmission system showed a similar relationship, with IC_{50} values of 0.23 and 0.09 μg/mL for clones 2 and 6, respectively (Figure 7).

Further studies of cell-cell transmission

It is possible that some of the resultant RLUs observed for the cell-cell transmission assay are due to cell-free virus being released from the producers and then infecting targets. To quantify this, prior to co-culturing the stable producers and targets, we removed increasing amounts of culture supernatant from the producers to infect the targets separately. We then co-cultured the producers and the targets. As can be seen in Figure S6D, there are some RLUs produced in the cell-free aspect of the experiment, but significantly less compared with the amount in the co-culture aspect of the experiment. These results are consistent with most of the RLUs in the cell-cell transmission assay coming from cell-cell and not cell-free transmission.

We also decided to construct producer cell lines expressing other S variants. We obtained codon-optimized versions of the Delta and Omicron variant S genes, both driven by the CMV IE enhancer/promoter. These cassettes were separately inserted into the base HIV-TV and stably introduced by transfection into 293T cells. A cell-cell transmission assay was performed in parallel with 293T-Spike-TV cells, which express Wuhan S. All three producer cell lines gave high RLUs, suggesting that this cell-cell transmission assay will work with S variants of concern as illustrated in Figure S6E.

DISCUSSION

Quantitative assays for the measurement of viral replication and infectivity are indispensable to future endeavors to develop prophylactic or therapeutic antiviral drugs or vaccines for SARS-CoV-2. We describe herein a cell-cell transmission assay that provides a quantitative readout to assess SARS-CoV-2 S-hACE2 interaction, in the absence of producing or using pseudotyped particles or live virus. At most this assay requires only BSL2 biocontainment and is very reliable, relatively rapid, and highly reproducible. The current gold standards for SARS-CoV-2 neutralization include pseudotyping using S and a suitable virus core encoding a reporter (Schmidt et al., 2020; Ou et al., 2020; Jiang et al., 2020; Zhao et al., 2021; Crawford et al., 2020) or inhibition of live virus replication *in vitro* or in animal models (Johansen et al., 2020; Bao et al., 2020; Zhao et al., 2021). Although it has been previously reported that inhibition of replication-competent virus or pseudotyped particles correlates well with protection from SARS-CoV-2 virus challenge in preclinical models of infection (Yu et al., 2020; Chandrashekar et al., 2020; Mercado et al., 2020), these assays necessitate higher level biocontainment and continued production, testing, and cryostorage of virus vector supernatants, which can be variable in quality and differ based on the laboratory. These assays may be time consuming, requiring several days to produce and concentrate pseudotyped particles to achieve high titer, with assay readout on susceptible cells after a few days (Quinonez and Sutton, 2002). This entire process typically may take a minimum of 7 days from the transfection of producer cells to the readout following transduction of the target cells with concentrated pseudoparticle vector supernatants, compared with this cell-cell transmission assay that takes a maximum of 4 days to complete. Hence, we thought it useful to develop this rapid, time-saving, cell-cell transmission assay that can be used to measure and quantify SARS-CoV-2 virus cell binding and entry to circumvent the challenges faced by the assays that are currently used as gold standards for SARS-CoV-2 neutralization.

Viruses can spread in a cell-free or a cell-associated manner, the latter involving direct cell-cell contact, also known as cell-cell transmission (Mothes et al., 2010). Currently, there is no direct evidence of cell-cell transmission in humans. On the other hand, it is not precisely clear how virus spread occurs, either *in vitro* or in vivo, whether it is cell-free, cell-associated, or due to cell fusion, although cell syncytia have been observed in the lung tissues of COVID-19+ patients (Bradley et al., 2020; Tian et al., 2020; Polak et al., 2020). Cell-cell transmission can occur via a virologic synapse and, at least in the case of HIV, is typically much more efficient than cell-free infection (Agosto et al., 2015;

Figure 6. Characterization and validation of the stable cell line system

(A–H) Ten-fold serial dilutions of LCB1 (A), 25-hydroxycholesterol (C), niclosamide (E), and 27-hydroxycholesterol (G) were pre-incubated with spike-expressing 293T producer cells for 1 h, and then hACE2-expressing target cells were added, performed in triplicate. RLU was measured at 48 h, and IC_{50} values were calculated for each serum. Results were compared with S pseudotyping assay for each compound: LCB1 (B), 25-hydroxycholesterol (D), niclosamide (F), and 27-hydroxycholesterol (H). See also Figures S5 and S6.

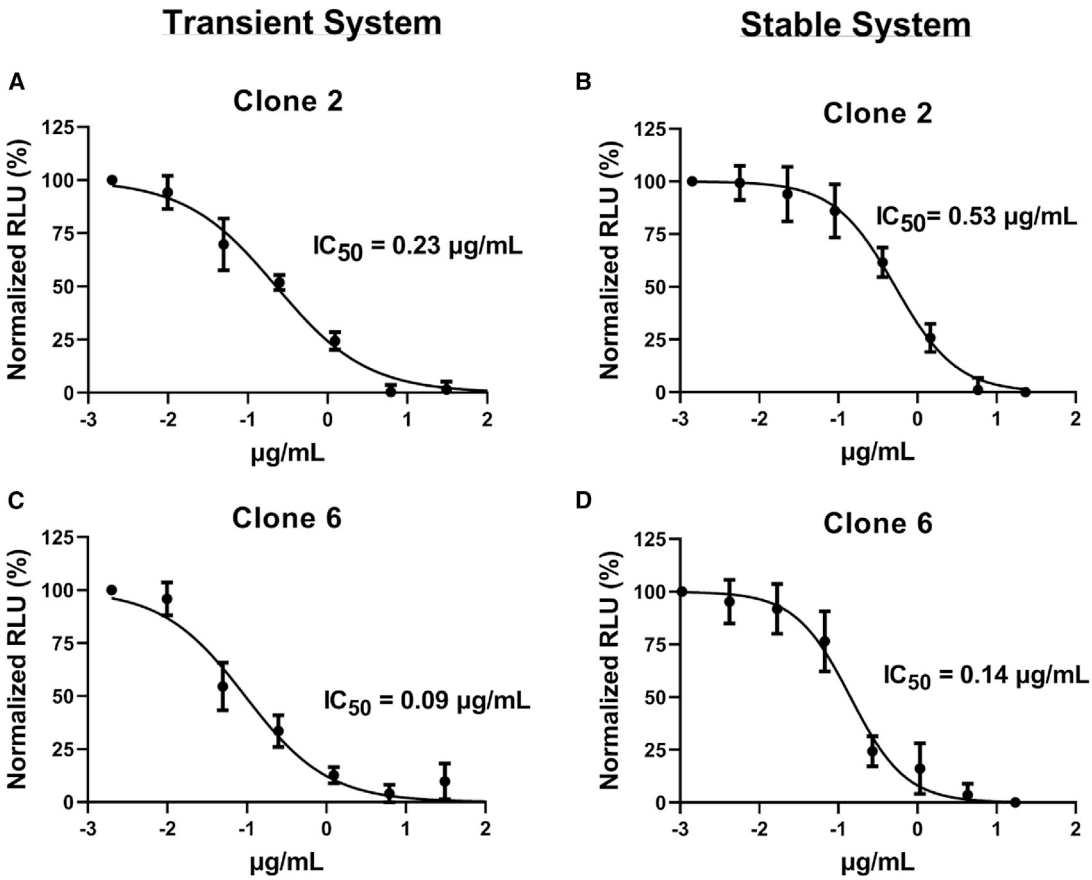

Figure 7. Anti-spike monoclonal antibodies inhibit cell-cell transmission

(A–D) Four-fold serial dilutions of monoclonal antibody were pre-incubated with spike-expressing producer cells for 1 h, and then hACE2-expressing target cells were added, performed in triplicate. RLU was measured after 48 h, and IC_{50} values were calculated. Clones 2 and 6 were assessed in the transient (A and C) and stable (B and D) cell-cell transmission assay.

Zhong et al., 2013a, 2013b; Jolly et al., 2010; Jolly and Sattentau, 2004; Martin et al., 2010; Abela et al., 2012). The ability of viruses to utilize and manipulate cell-cell contact likely contributes to the success of viral infections; cell-cell infection and spread not only facilitates rapid viral dissemination but may also promote immune evasion and influence disease progression (Zhong et al., 2013b; Aubert et al., 2009; Rudnicka et al., 2009). Whether any of the circulating S variants have enhanced cell-cell transmission is an open area of investigation. We developed a cell-cell transmission assay based on this concept, which is dependent on target cells expressing hACE2 and producer cells expressing S, along with all the requisite *trans*-acting factors for HIV core production (HIV-PV) and an HIV-based transfer vector, as illustrated in Figure 1C. Initial testing performed by transient transfection demonstrated that the assay is dependent on producer 293T cells expressing S, the transfer vector, and HIV-PV. The assay is also dependent on target cells expressing hACE2, with RLU numbers increasing ~10-fold when we used 293T-hACE2 versus unmodified 293T cells as targets. This is consistent with 293Ts expressing very low levels of hACE2 or a substitute receptor, as observed previously (Sun et al., 2021; Temmam et al., 2022).

Since transient transfection is relatively complex, occasionally unreliable, and not entirely amenable to high-throughput use, we sought to develop and successfully established stable cell lines that could be used to quantify cell-cell transmission rapidly and reliably, with highly reproducible and quantitative results. We thus generated a target cell line stably expressing hACE2 (293T-hACE2) and a producer cell line stably expressing S and the transfer vector, inGLUC (293T-Spike-TV), with HIV-PV introduced by transduction using HDAd-HIV-PV 24 h prior to target-producer cell co-culture. We titrated and optimized the HDAd-HIV-PV to use amounts that showed highest transduction efficiency with minimal to no cytopathic effect on the 293T cells. Of note, this HDAd can be propagated and amplified using a specialized helper adenovirus, such that the titers are more than 10^{12} vp/mL, and the HDAd is quite stable when cryostored for years at −80°C.

To further validate and characterize the cell-cell transmission assay, we tested the effects of convalescent sera and post-vaccination sera on cell-cell transmission of S in the transient and stable systems, comparing the results with pseudotyping. A robust positive correlation between cell-cell transmission and pseudotyping IC_{50} titers for both convalescent and

post-vaccination sera strongly suggests that the cell-cell transmission assay is indeed measuring S-hACE2 interaction and infectivity. Unsurprisingly, there was also a high correlation between the post-vaccination cell-cell transmission IC_{50} titers for the transient versus the stable system. The IC_{50} titers were generally higher with cell-cell transmission than those seen with pseudotyping, suggesting that S cell-cell transmission is more easily inhibited than cell-free transmission.

In addition to sera, we tested the effects of peptide LCB1 and small-molecule drugs, including cobicistat, niclosamide, apilimod, MPA, clofazimine, 25-hydroxycholesterol, and 27-hydroxycholesterol, all previously reported to be inhibitory of SARS-CoV-2 infection (Prabhakara et al., 2021; Xie et al., 2020; Yuan et al., 2021; Wang et al., 2020b). LCB1 has been reported to efficiently neutralize pseudotyped SARS-CoV-2 virus entry (Cao et al., 2020a), and we observed a similar effect on both pseudotyping and cell-cell transmission of Wuhan S. Comparison testing of peptide against the different S variants of concern (notably B.1.1.7, B.1.617.2, B.1.351, and B.1.1.529 https://www.who.int/en/activities/tracking-SARS-CoV-2-variants/) showed inhibition with variants B.1.1.7 and B.1.617.2, and to our surprise, no effect was seen with variants B.1.351 and B.1.1.529 at peptide concentrations similar to those shown in Figures S4A–S4D. Comparison testing of sera against the S variants of concern showed no substantial difference in the IC_{50} titers compared with Wuhan S (Figures S4E–S4L). Among the small molecules, only niclosamide, 25-hydroxycholesterol, and 27-hydroxycholesterol had significant effects on cell-cell transmission. Niclosamide was inhibitory, with an IC_{50} value of 0.10 μM, whereas both 25-hydroxycholesterol and 27-hydroxycholesterol were stimulatory in the stable cell line system, enhancing S-mediated cell-cell transmission with EC_{50} of 1.23 and 5.17 μM, respectively. These two cholesterol derivatives are both known to inhibit cholesterol biosynthesis and reduce cholesterol content in membranes; precisely how they would differentially affect cell-free versus cell-cell SARS-CoV-2 cell infection is uncertain at this juncture but worthy of further study.

We also tested murine anti-S monoclonal antibodies and tetherin. Tetherin is an interferon-induced membrane-associated protein whose expression is known to block the full release of HIV-1 and other enveloped viral particles from cells (Perez-Caballero et al., 2009). Tetherin showed a profound inhibitory effect against pseudotyped particles with an ~10-fold decrease in RLU when very low amounts were introduced into the producer cells. It had a less impressive effect on cell-cell transmission, with just an ~2-fold decrease in RLU at the highest normalized concentration of tetherin we tested (72 ng/cm^2), as illustrated in Figure S3. In general, it is felt that tetherin has a much greater impact on cell-free virus production, since the viruses produced remain attached to the producer cell and not released, whereas in the case of cell-cell transmission the large amount of extracellular virus present may counteract the inhibitory effect of the particle tethering, especially if the target is in contact with the producer cell. The impressive potency of the murine anti-S monoclonal antibodies in both cell-free and cell-cell transmission assays suggests that humanization of these antibodies for further evaluation, including clinical testing, may be of use.

This cell-cell transmission assay is also highly reproducible: repeated testing of an inhibitory peptide yielded very consistent results from three different experiments performed weeks apart, with minimal variation in IC_{50} values (Figure S2). Compared with pseudotyping, in which many laboratories use assorted plasmids to produce pseudotyped particles to titer on a range of targets using a variety of formats and readouts, here we employed just two stable cell lines and a single HDAd, the latter of which can be amplified to very high titer of $>10^{12}$ vp/mL. Thus, our cell-cell transmission assay, which is based on three relatively simple, readily available, and easily renewable reagents, should allow for facile comparisons when used by qualified investigators anywhere on the planet. The producer cell line was also easily modified to encode two S variants of concern that have emerged in the last 12 months.

In conclusion, we have developed and established a rapid, reliable, and reproducible SARS-CoV-2 S-hACE2 cell-cell transmission assay. The assay requires two stable cell lines that are well behaved and HDAd-HIV-PV, which has remarkable efficiency in transducing 293T cells. This assay does not require any specialized research reagents or laboratory equipment and should be easy to adapt for use in most investigative and clinical settings. It can be effectively used or modified for high-throughput screening for compounds and biologics that interfere with virus-cell binding and entry to complement other neutralization assays currently in use.

Limitations of the study

We attempted to make a stable cell line expressing HIV-PV; despite repeated efforts, we were unable to do so. Thus, at present we utilize an HDAd-HIV-PV that needs to be separately prepared. In the future we hope to modify the stable cell line to encode and express HIV-PV. In addition, as the pandemic continues, more S variants of concern are likely to arise; in each case we would need to construct a new stable producer cell line. Here, it took us roughly 6 weeks to make the Delta and Omicron S-encoding HIV transfer vectors and stably transfect and hygromycin B select the 293T cells and perform initial validation studies.

STAR★METHODS

Detailed methods are provided in the online version of this paper and include the following:

- KEY RESOURCES TABLE
- RESOURCE AVAILABILITY
  - Lead contact
  - Materials availability
  - Data and code availability
- EXPERIMENTAL MODEL AND SUBJECT DETAILS
  - Ethics statement
  - Cell lines
- METHOD DETAILS
  - Vectors and plasmids
  - Cell-cell transmission assay
  - X-gal staining for LacZ activity
  - *Gaussia* luciferase assay

- Pseudotyped virus neutralization assay
- Sera, LCB1, murine anti-spike monoclonal antibodies, small molecule drugs, and tetherin
- Time course experiment for LCB1
- Cell fusion assay
- Western blotting and nested PCR

- QUANTIFICATION AND STATISTICAL ANALYSIS

SUPPLEMENTAL INFORMATION

Supplemental information can be found online at https://doi.org/10.1016/j.crmeth.2022.100252.

ACKNOWLEDGMENTS

We thank Dr. Walther Mothes (Yale) and Matthew Wilson (Baylor College of Medicine) for generous reagent gifts. The following reagent was obtained through the NIH HIV Reagent Program, Division of AIDS, NIAID, NIH: Polyclonal Anti-Human Immunodeficiency Virus Immune Globulin, Pooled Inactivated Human Sera, ARP-3957, contributed by NABI and the National Heart Lung and Blood Institute (Dr. Luiz Barbosa). We thank the Yale IMPACT Research Team Membership for post-COVID-19 sera (Abeer Obaid, Akiko Iwasaki, Allison Nelson, Arnau Casanovas-Massana, Angela Nunez, Anjelica Martin, Bertie Geng, Codruta Todeasa, Denise Shepard, Elizabeth B. White, Erin Silva, Giuseppe De-Iuliis, Harold Rahming, Hong-Jai Park, Irene Matos, Jessica Nouws, Kadi-Ann Rose, Kelly Anastasio, Kristina Brower, Laura Glick, Lokesh Sharma, Maksym Minasyan, Maria Batsu, Maxine Kuang, Melissa Linehan, Michael H. Askenase, Mikhail Smolgovsky, Nicole Sonnert, Pavithra Vijayakumar, Santos Bermejo, Sofia Velazquez, Tyler Rice, William Khoury-Hanold, Xiaohua Peng, Yiyun Cao, John Fournier, M. Catherine Muenker, Adam J. Moore, Molly L. Bucklin, David McDonald, Camila Odio, and Yvette Strong). We also thank Ching Ying "Vanessa" Li for her work performing some GLUC assays. This work was supported in part by NIH grant R01 AI150334.

AUTHOR CONTRIBUTIONS

Conceptualization, G.S. and R.E.S.; methodology, G.S. and R.E.S.; validation, G.S. and M.K.; formal analysis, G.S. and R.E.S.; investigation, G.S., M.K., M.Z., and R.E.S.; resources, S.G., S.F.F., C.S.D.C., S.C., L.P., and P.R.; writing – original draft, G.S. and R.E.S.; writing – review & editing, G.S., S.G., and R.E.S.; visualization: R.E.S.; supervision, R.E.S.; project administration, R.E.S.; funding acquisition, R.E.S.

DECLARATION OF INTERESTS

The authors declare no competing interests.

Received: February 8, 2022
Revised: April 28, 2022
Accepted: June 14, 2022
Published: June 20, 2022

REFERENCES

Abela, I.A., Berlinger, L., Schanz, M., Reynell, L., Günthard, H.F., Rusert, P., and Trkola, A. (2012). Cell-cell transmission enables HIV-1 to evade inhibition by potent CD4bs directed antibodies. PLoS Pathog. *8*, e1002634. https://doi.org/10.1371/journal.ppat.1002634.

Agosto, L.M., Uchil, P.D., and Mothes, W. (2015). HIV cell-to-cell transmission: effects on pathogenesis and antiretroviral therapy. Trends Microbiol. *23*, 289–295. https://doi.org/10.1016/j.tim.2015.02.003.

Aubert, M., Yoon, M., Sloan, D.D., Spear, P.G., and Jerome, K.R. (2009). The virological synapse facilitates herpes simplex virus entry into T cells. J. Virol. *83*, 6171–6183. https://doi.org/10.1128/jvi.02163-08.

Bao, L.N., Deng, W., Huang, B.Y., Gao, H., Liu, J.N., Ren, L.L., Wei, Q., Yu, P., Xu, Y.F., Qi, F.F., et al. (2020). The pathogenicity of SARS-CoV-2 in hACE2 transgenic mice. Nature *583*, 830–833. https://doi.org/10.1038/s41586-020-2312-y.

Belouzard, S., Millet, J.K., Licitra, B.N., and Whittaker, G.R. (2012). Mechanisms of coronavirus cell entry mediated by the viral spike protein. Viruses-Basel *4*, 1011–1033. https://doi.org/10.3390/v4061011.

Bloch, E.M., Shoham, S., Casadevall, A., Sachais, B.S., Shaz, B., Winters, J.L., Van Buskirk, C., Grossman, B.J., Joyner, M., Henderson, J.P., et al. (2020). Deployment of convalescent plasma for the prevention and treatment of COVID-19. J. Clin. Invest. *130*, 2757–2765. https://doi.org/10.1172/JCI138745.

Bosch, B.J., Van Der Zee, R., De Haan, C.A.M., and Rottier, P.J.M. (2003). The coronavirus spike protein is a class I virus fusion protein: structural and functional characterization of the fusion core complex. J. Virol. *77*, 8801–8811. https://doi.org/10.1128/jvi.77.16.8801-8811.2003.

Bradley, B.T., Maioli, H., and Johnston, R. (2020). Histopathology and ultrastructural findings of fatal COVID-19 infections in Washington State: a case series. Lancet *396*, 320–332.

Cao, L.X., Goreshnik, I., Coventry, B., Case, J.B., Miller, L., Kozodoy, L., Chen, R.E., Carter, L., Walls, A.C., Park, Y.J., et al. (2020a). De novo design of picomolar SARS-CoV-2 miniprotein inhibitors. Science *370*, 426–431. https://doi.org/10.1126/science.abd9909.

Cao, Y., Su, B., Guo, X., Sun, W., Deng, Y., Bao, L., Zhu, Q., Zhang, X., Zheng, Y., Geng, C., et al. (2020b). Potent neutralizing antibodies against SARS-CoV-2 identified by high-throughput single-cell sequencing of convalescent patients' B cells. Cell *182*, 73–84.e16. https://doi.org/10.1016/j.cell.2020.05.025.

Casadevall, A., and Pirofski, L.A. (2020). The convalescent sera option for containing COVID-19. J. Clin. Invest. *130*, 1545–1548. https://doi.org/10.1172/jci138003.

Chan, J.F.W., Kok, K.H., Zhu, Z., Chu, H., To, K.K.W., Yuan, S., and Yuen, K.Y. (2020). Genomic characterization of the 2019 novel human-pathogenic coronavirus isolated from a patient with atypical pneumonia after visiting Wuhan. Emerg. Microbes Infect. *9*, 221–236. https://doi.org/10.1080/22221751.2020.1719902.

Chandrashekar, A., Liu, J., Martinot, A.J., Mcmahan, K., Mercado, N.B., Peter, L., Tostanoski, L.H., Yu, J., Maliga, Z., Nekorchuk, M., et al. (2020). SARS-CoV-2 infection protects against rechallenge in rhesus macaques. Science *369*, 812–817. https://doi.org/10.1126/science.abc4776.

Chen, P., Hübner, W., Spinelli, M.A., and Chen, B.K. (2007). Predominant mode of human immunodeficiency virus transfer between T cells is mediated by sustained Env-dependent neutralization-resistant virological synapses. J. Virol. *81*, 12582–12595. https://doi.org/10.1128/jvi.00381-07.

Coskun, A.K., Van Maanen, M., Nguyen, V., and Sutton, R.E. (2006). Human chromosome 2 carries a gene required for production of infectious human immunodeficiency virus type 1. J. Virol. *80*, 3406–3415. https://doi.org/10.1128/jvi.80.7.3406-3415.2006.

Crawford, K.H.D., Eguia, R., Dingens, A.S., Loes, A.N., Malone, K.D., Wolf, C.R., Chu, H.Y., Tortorici, M.A., Veesler, D., Murphy, M., et al. (2020). Protocol and reagents for pseudotyping lentiviral particles with SARS-CoV-2 spike protein for neutralization assays. Viruses *12*, 513. https://doi.org/10.3390/v12050513.

Graham, B.S. (2020). Rapid COVID-19 vaccine development. Science *368*, 945–946. https://doi.org/10.1126/science.abb8923.

Ho, H.L., Wang, F.Y., Lee, H.R., Huang, Y.L., Lai, C.L., Jen, W.C., Hsieh, S.L., and Chou, T.Y. (2020). Seroprevalence of COVID-19 in Taiwan revealed by testing anti-SARS-CoV-2 serological antibodies on 14, 765 hospital patients. Lancet Reg. Health West Pac. *3*, 100041. https://doi.org/10.1016/j.lanwpc.2020.100041.

Hoffmann, M., Kleine-Weber, H., Schroeder, S., Krüger, N., Herrler, T., Erichsen, S., Schiergens, T.S., Herrler, G., Wu, N.H., Nitsche, A., et al. (2020). SARS-CoV-2 cell entry depends on ACE2 and TMPRSS2 and is blocked by a clinically

proven protease inhibitor. Cell *181*, 271–280.e8. https://doi.org/10.1016/j.cell.2020.02.052.

Hu, Y., O'boyle, K., Palmer, D., Ng, P., and Sutton, R.E. (2015). High-level production of replication-defective human immunodeficiency type 1 virus vector particles using helper-dependent adenovirus vectors. Mol. Ther. Methods Clin. Dev. *2*, 15004. https://doi.org/10.1038/mtm.2015.4.

Huang, Y.X., Chen, Y.L., Li, S.P., Shen, J.P., Zuo, K., Zhou, S.C., and Chang, C. (2020). Development and validation of a simple-to-use nomogram for predicting the upgrade of atypical ductal hyperplasia on core needle biopsy in ultrasound-detected breast lesions. Front. Oncol. *10*, 609841. https://doi.org/10.3389/fonc.2020.609841.

Jiang, S., Hillyer, C., and Du, L. (2020). Neutralizing antibodies against SARS-CoV-2 and other human coronaviruses. Trends Immunol. *41*, 545. https://doi.org/10.1016/j.it.2020.04.008.

Johansen, M.D., Irving, A., Montagutelli, X., Tate, M.D., Rudloff, I., Nold, M.F., Hansbro, N.G., Kim, R.Y., Donovan, C., Liu, G., et al. (2020). Animal and translational models of SARS-CoV-2 infection and COVID-19. Mucosal Immunol. *13*, 877–891.

Jolly, C., Booth, N.J., and Neil, S.J.D. (2010). Cell-cell spread of human immunodeficiency virus type 1 overcomes tetherin/BST-2-mediated restriction in T cells. J. Virol. *84*, 12185–12199. https://doi.org/10.1128/jvi.01447-10.

Jolly, C., Kashefi, K., Hollinshead, M., and Sattentau, Q.J. (2004). HIV-1 cell to cell transfer across an Env-induced, actin-dependent synapse. J. Exp. Med. *199*, 283–293. https://doi.org/10.1084/jem.20030648.

Jolly, C., and Sattentau, Q.J. (2004). Retroviral spread by induction of virological synapses. Traffic *5*, 643–650. https://doi.org/10.1111/j.1600-0854.2004.00209.x.

Ju, B., Zhang, Q., Ge, J., Wang, R., Sun, J., Ge, X., Yu, J., Shan, S., Zhou, B., Song, S., et al. (2020). Human neutralizing antibodies elicited by SARS-CoV-2 infection. Nature *584*, 115–119. https://doi.org/10.1038/s41586-020-2380-z.

Klasse, P.J., and Moore, J.P. (2020). Antibodies to SARS-CoV-2 and their potential for therapeutic passive immunization. Elife *9*, e57877. https://doi.org/10.7554/elife.57877.

Li, G., Fan, Y., Lai, Y., Han, T., Li, Z., Zhou, P., Pan, P., Wang, W., Hu, D., Liu, X., et al. (2020a). Coronavirus infections and immune responses. J. Med. Virol. *92*, 424–432. https://doi.org/10.1002/jmv.25685.

Li, W.H., Moore, M.J., Vasilieva, N., Sui, J.H., Wong, S.K., Berne, M.A., Somasundaran, M., Sullivan, J.L., Luzuriaga, K., Greenough, T.C., et al. (2003). Angiotensin-converting enzyme 2 is a functional receptor for the SARS coronavirus. Nature *426*, 450–454. https://doi.org/10.1038/nature02145.

Li, Y., Zhou, W., Yang, L., and You, R. (2020b). Physiological and pathological regulation of ACE2, the SARS-CoV-2 receptor. Pharmacol. Res. *157*, 104833. https://doi.org/10.1016/j.phrs.2020.104833.

Liu, L., Wang, P., Nair, M.S., Yu, J., Rapp, M., Wang, Q., Luo, Y., Chan, J.F.W., Sahi, V., Figueroa, A., et al. (2020). Potent neutralizing antibodies against multiple epitopes on SARS-CoV-2 spike. Nature *584*, 450–456. https://doi.org/10.1038/s41586-020-2571-7.

Lorenz, T.C. (2012). Polymerase chain reaction: basic protocol plus troubleshooting and optimization strategies. J. Vis. Exp., e3998. https://doi.org/10.3791/3998.

Lythgoe, M.P., and Middleton, P. (2020). Ongoing clinical trials for the management of the COVID-19 pandemic. Trends Pharmacol. Sci. *41*, 363–382. https://doi.org/10.1016/j.tips.2020.03.006.

Martin, N., Welsch, S., Jolly, C., Briggs, J.A.G., Vaux, D., and Sattentau, Q.J. (2010). Virological synapse-mediated spread of human immunodeficiency virus type 1 between T cells is sensitive to entry inhibition. J. Virol. *84*, 3516–3527. https://doi.org/10.1128/jvi.02651-09.

Mazurov, D., Ilinskaya, A., Heidecker, G., Lloyd, P., and Derse, D. (2010a). Quantitative comparison of HTLV-1 and HIV-1 cell-to-cell infection with new replication dependent vectors. PLoS Pathog. *6*, e1000788. https://doi.org/10.1371/journal.ppat.1000788.

Mazurov, D., Ilinskaya, A., Heidecker, G., Lloyd, P., and Derse, D. (2010b). Quantitative comparison of HTLV-1 and HIV-1 cell-to-cell infection with new replication dependent vectors. PLoS Pathog. *6*, e1000788. https://doi.org/10.1371/journal.ppat.1000788.

Mercado, N.B., Zahn, R., Wegmann, F., Loos, C., Chandrashekar, A., Yu, J., Liu, J., Peter, L., Mcmahan, K., Tostanoski, L.H., et al. (2020). Single-shot Ad26 vaccine protects against SARS-CoV-2 in rhesus macaques. Nature *586*, 583–588. https://doi.org/10.1038/s41586-020-2607-z.

Mothes, W., Sherer, N.M., Jin, J., and Zhong, P. (2010). Virus cell-to-cell transmission. J. Virol. *84*, 8360–8368. https://doi.org/10.1128/jvi.00443-10.

Ou, X., Liu, Y., Lei, X., Li, P., Mi, D., Ren, L., Guo, L., Guo, R., Chen, T., Hu, J., et al. (2020). Characterization of spike glycoprotein of SARS-CoV-2 on virus entry and its immune cross-reactivity with SARS-CoV. Nat. Commun. *11*, 1620. https://doi.org/10.1038/s41467-020-15562-9.

Palmer, D., and Ng, P. (2003). Improved system for helper-dependent adenoviral vector production. Mol. Ther. *8*, 846–852. https://doi.org/10.1016/j.ymthe.2003.08.014.

Peng, L., Hu, Y., Mankowski, M.C., Ren, P., Chen, R.E., Wei, J., Zhao, M., Li, T., Tripler, T., Ye, L., et al. (2022). Monospecific and bispecific monoclonal SARS-CoV-2 neutralizing antibodies that maintain potency against B.1.617. Nat. Commun. *13*, 1638. https://doi.org/10.1038/s41467-022-29288-3.

Perez-Caballero, D., Zang, T., Ebrahimi, A., Mcnatt, M.W., Gregory, D.A., Johnson, M.C., and Bieniasz, P.D. (2009). Tetherin inhibits HIV-1 release by directly tethering virions to cells. Cell *139*, 499–511. https://doi.org/10.1016/j.cell.2009.08.039.

Pinto, D., Park, Y.J., Beltramello, M., Walls, A.C., Tortorici, M.A., Bianchi, S., Jaconi, S., Culap, K., Zatta, F., De Marco, A., et al. (2020). Cross-neutralization of SARS-CoV-2 by a human monoclonal SARS-CoV antibody. Nature *583*, 290–295. https://doi.org/10.1038/s41586-020-2349-y.

Polak, S.B., Van Gool, I.C., Cohen, D., Von Der Thusen, J.H., and Van Paassen, J. (2020). A systematic review of pathological findings in COVID-19: a pathophysiological timeline and possible mechanisms of disease progression. Mod. Pathol. *33*, 2128–2138.

Prabhakara, C., Godbole, R., Sil, P., Jahnavi, S., Gulzar, S.e.J., Van Zanten, T.S., Sheth, D., Subhash, N., Chandra, A., Shivaraj, A., et al. (2021). Strategies to target SARS-CoV-2 entry and infection using dual mechanisms of inhibition by acidification inhibitors. PLoS Pathog. *17*, e1009706. https://doi.org/10.1371/journal.ppat.1009706.

Quinonez, R., and Sutton, R.E. (2002). Lentiviral vectors for gene delivery into cells. DNA Cell Biol *21*, 937–951. https://doi.org/10.1089/104454902762053873.

Rehman, S.U., and Tabish, M. (2020). Alternative splicing of ACE2 possibly generates variants that may limit the entry of SARS-CoV-2: a potential therapeutic approach using SSOs. Clin. Sci. *134*, 1143–1150. https://doi.org/10.1042/cs20200419.

Riva, L., Yuan, S., Yin, X., Martin-Sancho, L., Matsunaga, N., Pache, L., Burgstaller-Muehlbacher, S., De Jesus, P.D., Teriete, P., Hull, M.V., et al. (2020). Discovery of SARS-CoV-2 antiviral drugs through large-scale compound repurposing. Nature *586*, 113–119. https://doi.org/10.1038/s41586-020-2577-1.

Rudnicka, D., Feldmann, J.R.M., Porrot, F.O., Wietgrefe, S., Guadagnini, S.P., Prévost, M.-C., Estaquier, J.R.M., Haase, A.T., Sol-Foulon, N., and Schwartz, O. (2009). Simultaneous cell-to-cell transmission of human immunodeficiency virus to multiple targets through polysynapses. J. Virol. *83*, 6234–6246. https://doi.org/10.1128/jvi.00282-09.

Sarma, P., Prajapat, M., Avti, P., Kaur, H., Kumar, S., and Medhi, B. (2020). Therapeutic options for the treatment of 2019-novel coronavirus: an evidence-based approach. Indian J. Pharmacol. *52*, 1. https://doi.org/10.4103/ijp.ijp_119_20.

Sattentau, Q. (2008). Avoiding the void: cell-to-cell spread of human viruses. Nat. Rev. Microbiol. *6*, 815–826. https://doi.org/10.1038/nrmicro1972.

Schmidt, F., Weisblum, Y., Muecksch, F., Hoffmann, H.-H., Michailidis, E., Lorenzi, J.C.C., Mendoza, P., Rutkowska, M., Bednarski, E., Gaebler, C., et al. (2020). Measuring SARS-CoV-2 neutralizing antibody activity using pseudotyped and chimeric viruses. J. Exp. Med. *217*, e20201181.

Shalhoub, S. (2020). Interferon beta-1b for COVID-19. Lancet *395*, 1670–1671. https://doi.org/10.1016/s0140-6736(20)31101-6.

Shang, J., Wan, Y.S., Luo, C.M., Ye, G., Geng, Q.B., Auerbach, A., and Li, F. (2020). Cell entry mechanisms of SARS-CoV-2. Proc. Natl. Acad. Sci. USA *117*, 11727–11734. https://doi.org/10.1073/pnas.2003138117.

Sun, G., Cui, Q., Garcia, G., Wang, C., Zhang, M., Arumugaswami, V., Riggs, A.D., and Shi, Y. (2021). Comparative transcriptomic analysis of SARS-CoV-2 infected cell model systems reveals differential innate immune responses. Scientific Rep. *11*, 17146. https://doi.org/10.1038/s41598-021-96462-w.

Suzuki, M., Cela, R., Clarke, C., Bertin, T.K., Mouriño, S., and Lee, B. (2010). Large-scale production of high-quality helper-dependent adenoviral vectors using adherent cells in cell factories. Hum. Gene Ther. *21*, 120–126. https://doi.org/10.1089/hum.2009.096.

Tada, T., Dcosta, B.M., Samanovic, M.I., Herati, R.S., Cornelius, A., Zhou, H., Vaill, A., Kazmierski, W., Mulligan, M.J., Landau, N.R., and Goff, S.P. (2021a). Convalescent-phase sera and vaccine-elicited antibodies largely maintain neutralizing titer against global SARS-CoV-2 variant spikes. mBio *12*, e0069621. https://doi.org/10.1128/mbio.00696-21.

Tada, T., Zhou, H., Dcosta, B.M., Samanovic, M.I., Mulligan, M.J., and Landau, N.R. (2021b). Partial resistance of SARS-CoV-2 Delta variants to vaccine-elicited antibodies and convalescent sera. iScience *24*, 103341. https://doi.org/10.1016/j.isci.2021.103341.

Tegally, H., Wilkinson, E., Giovanetti, M., Iranzadeh, A., Fonseca, V., Giandhari, J., Doolabh, D., Pillay, S., San, E.J., Msomi, N., et al. (2020). Emergence and rapid spread of a new severe acute respiratory syndrome-related coronavirus 2 (SARS-CoV-2) lineage with multiple spike mutations in South Africa. Preprint at medRxiv. https://doi.org/10.1101/2020.12.21.20248640.

Temmam, S., Vongphayloth, K., Baquero, E., Munier, S., Bonomi, M., Regnault, B., Douangboubpha, B., Karami, Y., Chrétien, D., Sanamxay, D., et al. (2022). Bat coronaviruses related to SARS-CoV-2 and infectious for human cells. Nature *604*, 330–336. https://doi.org/10.1038/s41586-022-04532-4.

Tian, S.F., Xiong, Y., Liu, H., Niu, L., Guo, J.C., Liao, M.Y., and Xiao, S.Y. (2020). Pathological study of the 2019 novel coronavirus disease (COVID-19) through postmortem core biopsies. Mod. Pathol. *33*, 1007–1014. https://doi.org/10.1038/s41379-020-0536-x.

VanPatten, S., He, M., Altiti, A., F Cheng, K., Ghanem, M.H., and Al-Abed, Y. (2020). Evidence supporting the use of peptides and peptidomimetics as potential SARS-CoV-2 (COVID-19) therapeutics. Future Med. Chem. *12*, 1647–1656. https://doi.org/10.4155/fmc-2020-0180.

Vogel, L. (2020). What's next now that the WHO has declared a COVID-19 pandemic? CMAJ *192*, E349–E350. https://doi.org/10.1503/cmaj.1095855.

Wang, H., Huang, Y., Hu, Q., Li, C., Liu, H., Wang, X., Li, W., Ma, W., Pu, Y., Du, Y., et al. (2020). A simulated dosimetric study of contribution to radiotherapy accuracy by fractional image guidance protocol of Halcyon system. Front. Oncol. *10*, 543147. https://doi.org/10.3389/fonc.2020.543147.

Wang, Q., and Zhang, L. (2020). Broadly neutralizing antibodies and vaccine design against HIV-1 infection. Front. Med. *14*, 30–42. https://doi.org/10.1007/s11684-019-0721-9.

Wang, S., Li, W., Hui, H., Tiwari, S.K., Zhang, Q., Croker, B.A., Rawlings, S., Smith, D., Carlin, A.F., and Rana, T.M. (2020b). Cholesterol 25-Hydroxylase inhibits SARS-CoV-2 and other coronaviruses by depleting membrane cholesterol. EMBO J. *39*, e106057. https://doi.org/10.15252/embj.2020106057.

Wrapp, D., Wang, N.S., Corbett, K.S., Goldsmith, J.A., Hsieh, C.L., Abiona, O., Graham, B.S., and Mclellan, J.S. (2020). Cryo-EM structure of the 2019-nCoV spike in the prefusion conformation. Science *367*, 1260–1263. https://doi.org/10.1126/science.abb2507.

Wu, F., Zhao, S., Yu, B., Chen, Y.M., Wang, W., Song, Z.G., Hu, Y., Tao, Z.W., Tian, J.H., Pei, Y.Y., et al. (2020a). A new coronavirus associated with human respiratory disease in China. Nature *579*, 265–269. https://doi.org/10.1038/s41586-020-2008-3.

Wu, Y., Li, C., Xia, S., Tian, X., Kong, Y., Wang, Z., Gu, C., Zhang, R., Tu, C., Xie, Y., et al. (2020b). Identification of human single-domain antibodies against SARS-CoV-2. Cell Host Microbe *27*, 891–898.e5. https://doi.org/10.1016/j.chom.2020.04.023.

Xie, X., Muruato, A.E., Zhang, X., Lokugamage, K.G., Fontes-Garfias, C.R., Zou, J., Liu, J., Ren, P., Balakrishnan, M., Cihlar, T., et al. (2020). A nanoluciferase SARS-CoV-2 for rapid neutralization testing and screening of anti-infective drugs for COVID-19. Nat. Commun. *11*, 5214. https://doi.org/10.1038/s41467-020-19055-7.

Yu, J., Tostanoski, L.H., Peter, L., Mercado, N.B., Mcmahan, K., Mahrokhian, S.H., Nkolola, J.P., Liu, J., Li, Z., Chandrashekar, A., et al. (2020). DNA vaccine protection against SARS-CoV-2 in rhesus macaques. Science *369*, 806–811. https://doi.org/10.1126/science.abc6284.

Yuan, S., Yin, X., Meng, X., Chan, J.F.-W., Ye, Z.-W., Riva, L., Pache, L., Chan, C.C.-Y., Lai, P.-M., Chan, C.C.-S., et al. (2021). Clofazimine broadly inhibits coronaviruses including SARS-CoV-2. Nature *593*, 418–423. https://doi.org/10.1038/s41586-021-03431-4.

Zeng, C., Evans, J.P., Pearson, R., Qu, P., Zheng, Y.M., Robinson, R.T., Hall-Stoodley, L., Yount, J., Pannu, S., Mallampalli, R.K., et al. (2020). Neutralizing antibody against SARS-CoV-2 spike in COVID-19 patients, health care workers, and convalescent plasma donors. JCI Insight *5*, 143213. https://doi.org/10.1172/jci.insight.143213.

Zhang, Y., Chapman, J.H., Ulcay, A., and Sutton, R.E. (2019). Neutralization synergy between HIV-1 attachment inhibitor fostemsavir and anti-CD4 binding site broadly neutralizing antibodies against HIV. J. Virol. *93*, e01446-18. https://doi.org/10.1128/jvi.01446-18.

Zhao, M., Su, P.-Y., Castro, D.A., Tripler, T.N., Hu, Y., Cook, M., Ko, A.I., Farhadian, S.F., Israelow, B., Dela Cruz, C.S., et al. (2021). Rapid, reliable, and reproducible cell fusion assay to quantify SARS-Cov-2 spike interaction with hACE2. PLoS Pathog. *17*, e1009683. https://doi.org/10.1371/journal.ppat.1009683.

Zhong, P., Agosto, L.M., Ilinskaya, A., Dorjbal, B., Truong, R., Derse, D., Uchil, P.D., Heidecker, G., and Mothes, W. (2013a). Cell-to-cell transmission can overcome multiple donor and target cell barriers imposed on cell-free HIV. PLoS One *8*, e53138. https://doi.org/10.1371/journal.pone.0053138.

Zhong, P., Agosto, L.M., Munro, J.B., and Mothes, W. (2013b). Cell-to-cell transmission of viruses. Curr. Opin. Virol. *3*, 44–50. https://doi.org/10.1016/j.coviro.2012.11.004.

Zhou, G., and Zhao, Q. (2020). Perspectives on therapeutic neutralizing antibodies against the Novel Coronavirus SARS-CoV-2. Int. J. Biol. Sci. *16*, 1718–1723. https://doi.org/10.7150/ijbs.45123.

Zost, S.J., Gilchuk, P., Case, J.B., Binshtein, E., Chen, R.E., Nkolola, J.P., Schäfer, A., Reidy, J.X., Trivette, A., Nargi, R.S., et al. (2020). Potently neutralizing and protective human antibodies against SARS-CoV-2. Nature *584*, 443–449. https://doi.org/10.1038/s41586-020-2548-6.

STAR★METHODS

KEY RESOURCES TABLE

REAGENT or RESOURCE	SOURCE	IDENTIFIER
Antibodies		
Goat anti-hACE2	R&D systems	Cat# AF933-SP
Mouse anti-FLAG	Sigma-Aldrich	Cat# F1804-50UG
Rabbit anti-goat-HRP	Sigma-Aldrich	Cat# AP106P
Rabbit anti-mouse HRP	Cell Signaling	Cat# 58802
Goat anti-rabbit HRP	Sigma-Aldrich	Cat# 12-348
Rabbit anti-GAPDH	Sigma-Aldrich	Cat# SAB5600208
Anti-human HRP	Sigma-Aldrich	Cat# AP112P
Anti-HIV human sera	NIH AIDS Reagent Repository	Cat# 3957
Biological samples		
Murine anti-spike monoclonal antibodies	Sidi Chen	https://doi.org/10.1038/s41467-022-29288-3
Post-vaccine sera	West Haven VA Medical Center	N/A
Convalescent Sera	YNHH hospital (IMPACT research team)	N/A
Chemicals, peptides, and recombinant proteins		
Coelenterazine	Gold Bio	CAS #55779-48-1
Sodium Iodide	Sigma-Aldrich	CAS #7681-82-5
Deposited data		
Raw and Analyzed Data	Mendeley Data	https://doi.org/10.17632/m7twyzc4yj.3
Experimental models: Cell lines		
Human Embryonic Kidney 293T cells	ATCC	Cat# CRL-3216
293T-Spike-HIV-TV	This paper	N/A
293T-hACE2	This paper	N/A
Oligonucleotides		
LCB1 peptide (56-mer) DKEWILQKIYEIMRLLDELGHAEASMR VSDLIYEFMKKGDERLLEEAERLLEEVER	ABI Scientific Inc	Sequence ID: 206841
Nested PCR; Inside-Reverse primer: 5′-GCAGTGAGCGCAACGCAATTAATGTGA-3′	This paper	N/A
Nested PCR; Outside-Reverse primer: 5′-GCGTTGGCCGATTCATTAATGCAGCT-3′	This paper	N/A
Nested PCR; Outside-Forward primer: 5′-TTCATGCCTTCTTCTCTTTCCTACAGGGG-3′	This paper	N/A
Nested PCR; Inside-Forward primer: 5′-GGCCACGATGTTGAAGTCTTCGTTGTTC-3′	This paper	N/A
Recombinant DNA		
pHIV-CMV-hACE2-IRES-Puro	This paper	N/A
pT-PB-SARS-CoV-2-Spike-IRES-Blasti	This paper	N/A
pUCHR-inGLuc-Beta	Walther Mothes	https://doi.org/10.1371/journal.pone.0053138
pUCHR-inGLuc-pgk-hygro	This paper	N/A
Software and algorithms		
GraphPad Prism 9.3.1	GraphPad Software	https://www.graphpad.com/scientific-software/prism/

(*Continued on next page*)

Continued

REAGENT or RESOURCE	SOURCE	IDENTIFIER
Other		
HDAd-HIV-PV	This paper	N/A
Clofazimine	Sigma-Aldrich	Cas# 2030-63-9
Cobicistat	Sigma-Aldrich	Cas# 1004316-88-4
Apilimod	Sigma-Aldrich	Cas# 541550-19-0
Mycophenolate	Sigma-Aldrich	Cas# 128794-94-5
Niclosamide	Sigma-Aldrich	Cas# 50-65-7
27-hydroxycholesterol	Sigma-Aldrich	Cas# 20380-11-4
25-hydroxycholesterol	Sigma-Aldrich	Cas# 2140-46-7

RESOURCE AVAILABILITY

Lead contact

Further information and requests for resources and reagents should be directed to and will be fulfilled by the lead contact, Dr. Richard Sutton (richard.sutton@yale.edu).

Materials availability

Plasmids and the stable cell lines generated during this study are available from the lead contact upon request.

Data and code availability

All the Raw datasets generated during this study have been deposited at Mendeley Data and are publicly available as of the date of publication. DOIs are listed in the key resources table.

This paper does not report original code.

Any additional information required to reanalyze the data reported in this paper is available from the lead contact upon request.

EXPERIMENTAL MODEL AND SUBJECT DETAILS

Ethics statement

Deidentified COVID-19+ convalescent sera samples were obtained from YNHH hospital (IMPACT research team). IMPACT study was approved by the Yale University institutional review board (IRB). Deidentified Post-vaccine serum samples were obtained from West Haven VA Medical Center (approved by both the Yale IRB and WHVA IRB). Written, informed consent was obtained and documented for all subjects. Convalescent sera from 11 COVID-19+ patients and sera from 11 subjects at one month post vaccination were selected at random for testing. Demographic and relevant clinical information of the subjects is shown in Tables S1 and S2 for convalescent and post-vaccine sera, respectively.

Cell lines

Human embryonic kidney cell line 293T (#CRL-3216), was originally purchased from ATCC. Cell lines were maintained in Dulbecco's modified Eagle's high-glucose medium supplemented with 10% fetal calf serum, penicillin, streptomycin, and 10 μg/mL of ciprofloxacin (complete DMEM), with other antibiotics or supplements as indicated in the text. Cells were grown in 5% CO_2, 37°C water-jacketed incubators and passaged every 3 to 5 days.

METHOD DETAILS

Vectors and plasmids

CMV-driven expression plasmid for S with an FLAG tag at the COOH terminus (pcDNA-SARS-CoV-2-S) was as previously described, as was plasmid encoding human ACE2 (hACE2) (Zhao et al., 2021). The hACE2 2.6 kbp ORF was blunt-cloned into a third generation HIV vector 3′ of CMV promoter and 5′ of an IRES-puro^r cassette to generate pHIV-CMV-hACE2-IRES-Puro. pSV-Tat, pCMV-Tat, and pLTR-LUC were as previously described (Zhao et al., 2021). Full length codon optimized Spike (S) was used in the development of this assay, S from pcDNA-SARS-CoV-2-S was inserted into a *piggybac* transposon (originally obtained from Matt Wilson of Baylor, along with the transposase plasmid pCMV-*piggybac*) that had been modified to encode a CMV-IRES-*bsd*^{r} cassette; resultant plasmid was named pT-PB-SARS-CoV-2-Spike-IRES-Blasti. HIV-TV plasmid, encoding the intron-regulated HIV-based *Gaussia* luciferase pUCHR-inGLuc-Beta (HIV-inGLuc), was obtained from Dr. Walther Mothes, originally generated in the Derse/Heidecker

lab as previously described (Mazurov et al., 2010a). Transcription of GLuc is antisense relative to transcription of the viral genomic RNA and is interrupted by a γ-globin intron inserted in sense orientation relative to the genomic RNA (Zhong et al., 2013a); this plasmid was modified to encode a hygromycin B^r expression cassette (pUCHR-inGLuc-pgk-hygro). Plasmid expressing human tetherin, pcDNA3.1-tetherin, was also from Dr. Walther Mothes. HIV-PV was as described (Hu et al., 2015). HDAd-HIV-PV was produced as previously described (Suzuki et al., 2010; Coskun et al., 2006; Palmer and Ng, 2003). Variant B.1.1.7-expressing plasmid was obtained from Dr. Walther Mothes; it is codon-optimized and contains eight S protein amino acid mutations (Δ69-70, Y144Del, N501Y, A570D, P681H, T716I, S982A and D1118H) in addition to D614G (Tada et al., 2021a). B.1.351 variant was initially isolated in South Africa and has nine S protein amino acid mutations (L18F, D80A, D215G, L242-244del, R246I, K417N, E484K, N501Y and A701V) three of which (K417N, E484K and N501Y) are in the receptor binding domain (RBD) (Tegally et al., 2020). To construct this variant the latter three mutations were introduced into pcDNA-SARS-CoV-2-S using gene synthesis. Variant B.1.617.2 was initially isolated in India, its spike protein has L452R and T478K mutations in the RBD in addition to D614G and a P681R mutation near the proteolytic processing site (Tada et al., 2021b). To construct this VOC, L452R and T478K were introduced into pcDNA-SARS-CoV-2-S using gene synthesis. Codon-optimized Delta S variant plasmid was from the Mothes' lab; codon-optimized Omicron S variant plasmid was originally purchased from Sino-Biological.

Cell-cell transmission assay

To measure cell-cell transmission of SARS CoV-2, we employed a system developed by the late David Derse (Mazurov et al., 2010b). In one cell (the target cell), hACE2 was stably introduced by VSV G-mediated HIV-based transduction using pHIV-CMV-hACE2-IRES-Puro to produce target HEK 293T-hACE2 cells, maintained in selection using 10 μg/mL puromycin (Sigma-Aldrich). From Walther Mothes we obtained a second-generation cell-cell transmission HIV-TV, in which an improved intron in the forward orientation was used to disrupt a backwards *Gaussia* luciferase that is secreted from infected cells. For the transient cell-cell transmission assay this HIV-TV, inGLUC, was transiently co-transfected into 293T cells along with S and HIV-PV. After 48 h these cells were mixed 1:1 with 293T-hACE2 cells, and 48 h later cell culture supernatant was removed to measure *Gaussia* luciferase activity.

For the stable system, producer 293T cells were made by first transfecting linearized pUCHR-inGLuc-pgk-hygro using calcium phosphate co-precipitation method and selecting stably transfected cells using 200–400 μg/mL hygromycin B (Calbiochem). Next, linearized pT-PB-SARS-CoV-2-Spike-IRES-Blasti was co-transfected along with *piggybac* transposase using calcium phosphate co-precipitation method and S-modified cells were selected in both blasticidin (10 μg/mL; GoldBio) and hygromycin B (200 μg/mL; Calbiochem). To express HIV-PV, 2×10^5 stable producer 293T-Spike-TV cells were seeded in a 12-well format and transduced with 40 nL of concentrated HDAd-HIV-PV (Hu et al., 2015) at an MOI of ~4 IU/cell. At 24 h post-transduction cells were refed with fresh media, then harvested after another 24 h and co-cultured at ratio of 1:1 with target 293T-hACE2 cells. For both the stable and transient systems, cells were co-cultured in triplicate in 0.2 mL of complete DMEM per well in a 96-well format. After 48 h cell culture supernatant was harvested and assayed for *Gaussia* luciferase activity.

The Delta and Omicron S DNA cassettes, both CMV IE/promoter-driven, were separately blunt-end ligated into pUCHR-inGLuc-pgk-hygro into a unique Sfi1 restriction site downstream of the 3′ LTR; cloning details are available upon request. These two plasmids were linearized and individually transfected into 293T cells using the calcium-phosphate method, and stably transfected cells were selected using hygromycin B as described above.

X-gal staining for LacZ activity

2×10^5 293T- Spike-TV cells were seeded in a 12-well format then transduced with increasing amounts of HDAd-HIV-PV as indicated. At 24 h cells were refed with fresh complete DMEM media, incubated further for 24 h and then fixed with 4% paraformaldehyde in phosphate buffered saline (PBS) for 10 min. X-gal staining solution (1 mg/mL X-gal from Gold Bio, 6 mM potassium ferrocyanide, and 6 mM potassium ferricyanide in PBS) was incubated with fixed cells for 24 h before plates were washed with PBS and photographs taken.

Gaussia luciferase assay

Gaussia luciferase (GLUC) assay buffer was prepared using 10 μM coelenterazine (Gold Bio), 50 mM Sodium Iodide (Sigma-Aldrich) in phosphate-buffered saline (PBS). 100 μL of culture supernatant was harvested from the co-cultured cells as described above and transferred into a white 96-well microplate to which 100 μL of the GLUC assay buffer was present. RLU was quantified on a Biotek plate reader. Data was analyzed with non-linear regression using GraphPad Prism to generate neutralization curves and IC-50 values.

Pseudotyped virus neutralization assay

Pseudotyped HIV-FFLUC was produced as previously described (Zhang et al., 2019) using pcDNA-SARS-CoV-2-S (Zhao et al., 2021). Pseudotyped particles were concentrated by ultracentrifugation. Convalescent and post-vaccine sera, monoclonal antibodies, and LCB1 were serially diluted as indicated and pre-incubated with S-pseudotyped particles for 1 h at 37°C then added to 293T-hACE2 target cells in 96-well format. After an overnight incubation fresh medium was added. After another 48 h cells were lysed and RLU measured as described previously (Zhao et al., 2021). IC-50 values were calculated using GraphPad Prism software. Non-linear regression with normalized response model was applied.

Sera, LCB1, murine anti-spike monoclonal antibodies, small molecule drugs, and tetherin

COVID-19 + convalescent sera were obtained from YNHH hospital (IMPACT research team). Post-vaccine sera were obtained from West Haven VA Medical Center. 56-mer peptide LCB1 was as previously described (Zhao et al., 2021) and stored at −80°C prior to use. Clofazimine, cobicistat, apilimod, niclosamide, 25-hydroxycholesterol, 27-hydroxycholesterol, and mycophenolate were purchased from Sigma-Aldrich. Murine anti-spike monoclonal antibodies, clones 2 and 6 were a gift of Sidi Chen and were as previously described (Peng et al., 2022). Producer and target 293T cells were generated as described above. Producer cells were harvested 48 h post-transfection or transduction for the transient or stable system, respectively. 4×10^4 producer cells were resuspended in 50 μL complete DMEM per well in 96-well plates. Serially diluted amounts of anti-spike mAbs, sera, LCB1, or small molecule drugs were then added to producer cells and incubated at 37°C for 1 h, then an equal amount of target cells in 50μL were added per well. The cells were co-cultured at 37°C, after 48 h supernatants were harvested and *Gaussia* luciferase activity measured as described above. Studies with tetherin were done by transiently transfecting the producer 293T cells with increasing amounts of tetherin expression plasmid DNA in 12-well format for cell-cell transmission. After 48 h cells were co-cultured with target 293T-hACE2 cells and supernatants harvested after 48 h of GLUC activity measured as described above.

Time course experiment for LCB1

96-well plates were seeded with 4×10^4 producer 293T cells in 100 μL per well. 10-fold serially diluted LCB1 was added at −1, 0, +1 and +2 h relative to the addition of 293T-hACE2 targets. After 48 h GLUC activity was measured as described above.

Cell fusion assay

HOS cells stably expressing HIV Tat and hACE2 were mixed 1:1 with TZMbl cells stably expressing S as described (Zhao et al., 2021). At 48 h transfected cells were lifted, mixed 1:1, and after another 16–24 h cells were lysed and RLU measured by plate reader in 96-well format as described (Zhao et al., 2021).

Western blotting and nested PCR

Expression of hACE2, S, and HIV Gag proteins in the stable 293T cells was confirmed by immunoblotting. Cells were lysed using RIPA buffer. Samples were boiled for 10 min in the presence of SDS and DTT, size-separated on pre-made SDS-PAGE gradient gels (Bio-Rad) and transferred onto PVDF filter membranes as previously described (Zeng et al., 2020). hACE2 and S were detected by goat anti-hACE2 (R&D systems) and mouse anti-FLAG (Sigma-Aldrich) primary antibodies and rabbit anti-goat-HRP (Sigma-Aldrich) and rabbit anti-mouse HRP (Cell Signaling) secondary antibodies, respectively. Gag-pol protein expression was detected by using anti-HIV human sera as primary antibody (#3957 from NIH AIDS Reagent Repository) and anti-human HRP secondary antibody (Sigma-Aldrich). In parallel cellular GAPDH was detected by immunoblotting using rabbit anti-GAPDH primary antibody (Sigma-Aldrich) and goat anti-rabbit HRP secondary antibody (Sigma-Aldrich).

To confirm presence of the HIV transfer vector in the stable cell line, nested PCR was performed as previously described (Lorenz, 2012), using extracted genomic DNA as template and size-separating DNA products by horizontal agarose gel electrophoresis.

QUANTIFICATION AND STATISTICAL ANALYSIS

All statistical analyses were conducted using GraphPad Prism 9.3.1. Luciferase assays were performed, and luciferase expression quantified, in triplicate as indicated in the figure legends with the mean being the average value of the three readings. In all the experiments, data are represented as the mean ± SD. The significance of the differences between the groups was analyzed with paired t-test. p values < 0.05 were considered statistically significant. The specific p value is depicted in the respective figure panel.

Cell Reports Methods, Volume *2*

Supplemental information

Development of an efficient reproducible cell-cell transmission assay for rapid quantification of SARS-CoV-2 spike interaction with hACE2

George Ssenyange, Maya Kerfoot, Min Zhao, Shelli Farhadian, Sidi Chen, Lei Peng, Ping Ren, Charles S. Dela Cruz, Shaili Gupta, and Richard E. Sutton

SUPPLEMENTAL INFORMATION

SUPPLEMENTAL FIGURES AND LEGENDS

Figure S1. Neutralization curves for post-vaccine and convalescent sera showing inhibition of S pseudotyped particle infection. Four-fold serial dilutions of convalescent (**A-C**) and post-vaccine (**E-G**) sera were pre-incubated with S pseudotyped particles for 1 h, then added to 293T-hACE2 target cells in triplicate. RLU was measured after 48 h, and IC-50 values calculated. One convalescent and one post-vaccine sample showed no significant inhibitory effect (**D & H**, respectively). Related to Figures 2, 3 and 5.

Figure S2. Reproducibility of cell-cell transmission assay. (**A-C**) Inhibition of cell-cell transmission by LCB1 performed 3 different times many weeks apart, IC-50 values were calculated for each experiment. (**D**) IC-50 values for the 3 experiments including the average IC-50 +/- SD. 1% DMSO in PBS was used as control. **(E, F)** Time-of-addition experiment using LCB1 to inhibit virus infection: 10-fold serial dilutions of LCB1 were added at -1, 0, +1 and +2 h relative to target cell addition. **(E)** pseudotyping; **(F)** cell-cell transmission. Related to Figure 6

Figure S3. Effect of tetherin on virus infection. Increasing amounts of tetherin plasmid DNA transfected into producer 293T cells (12-well plate for cell-cell transmission and 10 cm plate format for pseudotyping) inhibited cell-cell transmission of S **(A)** and VSV G **(B),** with a more profound inhibitory effect seen with pseudotyping with S **(B)** and VSV G **(D),** relative to cell-cell transmission. Effect of cholesterol derivatives on VSV G cell-cell transmission in transiently transfected cells: 10-fold serial dilutions of 25-hydroxycholesterol **(E)** and 27-hydroxycholesterol **(F)** were pre-incubated with VSV G-expressing producer cells for 1 hour; 293T target cells were then added, performed in triplicate, with RLU readout at 48 h. ns denotes not significant; *p-value <0.05; **p-value<0.01. Related to Figure 6.

Figure S4. Studies with S variants of concern (VOC). Serial dilutions of convalescent sera, post-vaccine sera, and peptide LCB1 were pre-incubated for 1 h with 293T producer cells transiently transfected with the different S VOC along with HIV-PV and

HIV-TV; 293T-hACE2 target cells were then added in triplicate and RLU measured at 48 h. **(A&C)** LCB1 inhibits cell-cell transmission of S VOC B.1.1.7 **(A)** and B.1.617.2 **(C)** but not B.1.351 **(B). (D-F)** Convalescent sera inhibits cell-cell transmission of spike VOCs. **(G-I)** Post-vaccine sera inhibits cell-cell transmission of S VOCs. Related to Figures 2, 3 and 4.

Figure S5. Immunoblotting and PCR of stable cell lines. (A-D) Expression of S, HIV Gag, and hACE2 proteins in stable cell lines were confirmed by Western blotting, with GAPDH immunoblots performed in parallel**. (E)** Confirmation of presence of HIV-TV by PCR. Ethidium bromide-stained horizontal agarose gel showing PCR product to confirm stable introduction of HIV-TV (inGLUC) in the 293T-Spike-TV stable producer cell line. Nested PCR was performed on extracted genomic DNA from 293T cells transiently and stably expressing HIV-TV. Related to Figures 5 and 6

Figure S6. Transduction of stable 293T cells with HDAd-HIV-PV. (A-B) 293T-Spike-TV cells were transduced with increasing amounts HDAd-HIV-PV as indicated, performed in 12-well format, fixed, and stained using X-gal for lacZ expression. **(A)** Microscopy; **(B)** Photograph of actual plate. **(C)** Stable 293T-Spike-TV producer cells were transduced with indicated amounts of concentrated HDAd-HIV-PV; after 24 h cells were refed, co-cultured with 293T-hACE2 target cells in triplicate, and RLU measured after 48 h. **(D)** Stable 293T-Spike-TV producer cells were transduced HDAd-HIV-PV, at 48 h culture supernatant were harvested and used to transduce 293T-hACE2 target cells, pre-seeded the previous day in a separate plate, with indicated amounts of the supernatant and RLU measured at 48 h. Results normalized to µL/50,000 target cells. A positive control with producer cells directly co-cultured with the targets was included. **(E)** Stable 293T-Spike-TV producer cells expressing different spike variants of concern, as indicated, were transduced with HDAd-HIV-PV; after 24 h cells were refed, co-cultured with 293T-hACE2 target cells in triplicate, and RLU measured after 48 h. Transduction and luciferase assays were performed in 3 independent experiments; the mean and SD are shown. Related to Figures 5 and 6.

Figure S1. Neutralization curves for post-vaccine and convalescent sera showing inhibition of S pseudotyped particle infection. Related to Figures 2, 3 and 5.

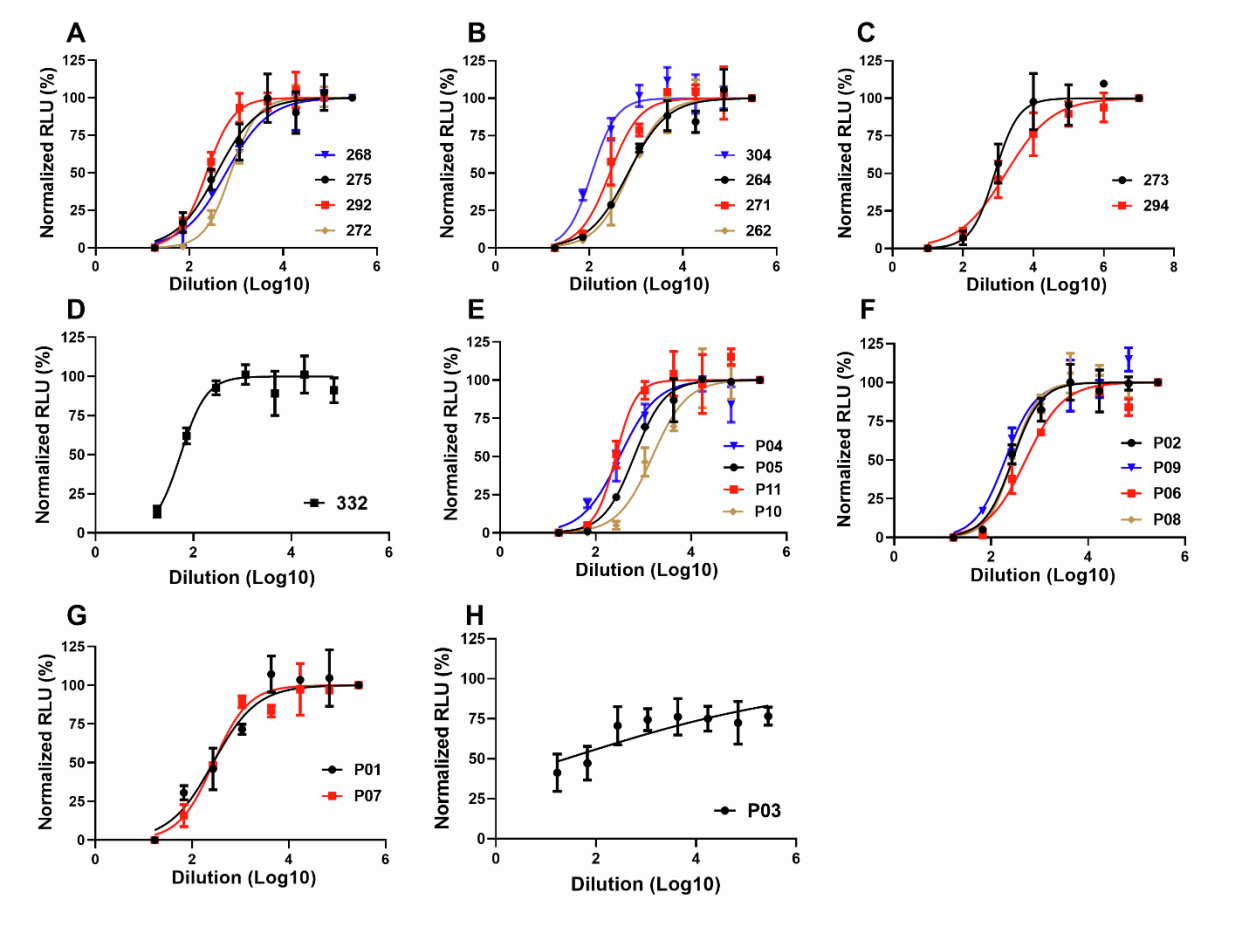

Figure S2. Reproducibility of cell-cell transmission assay. Related to Figure 6

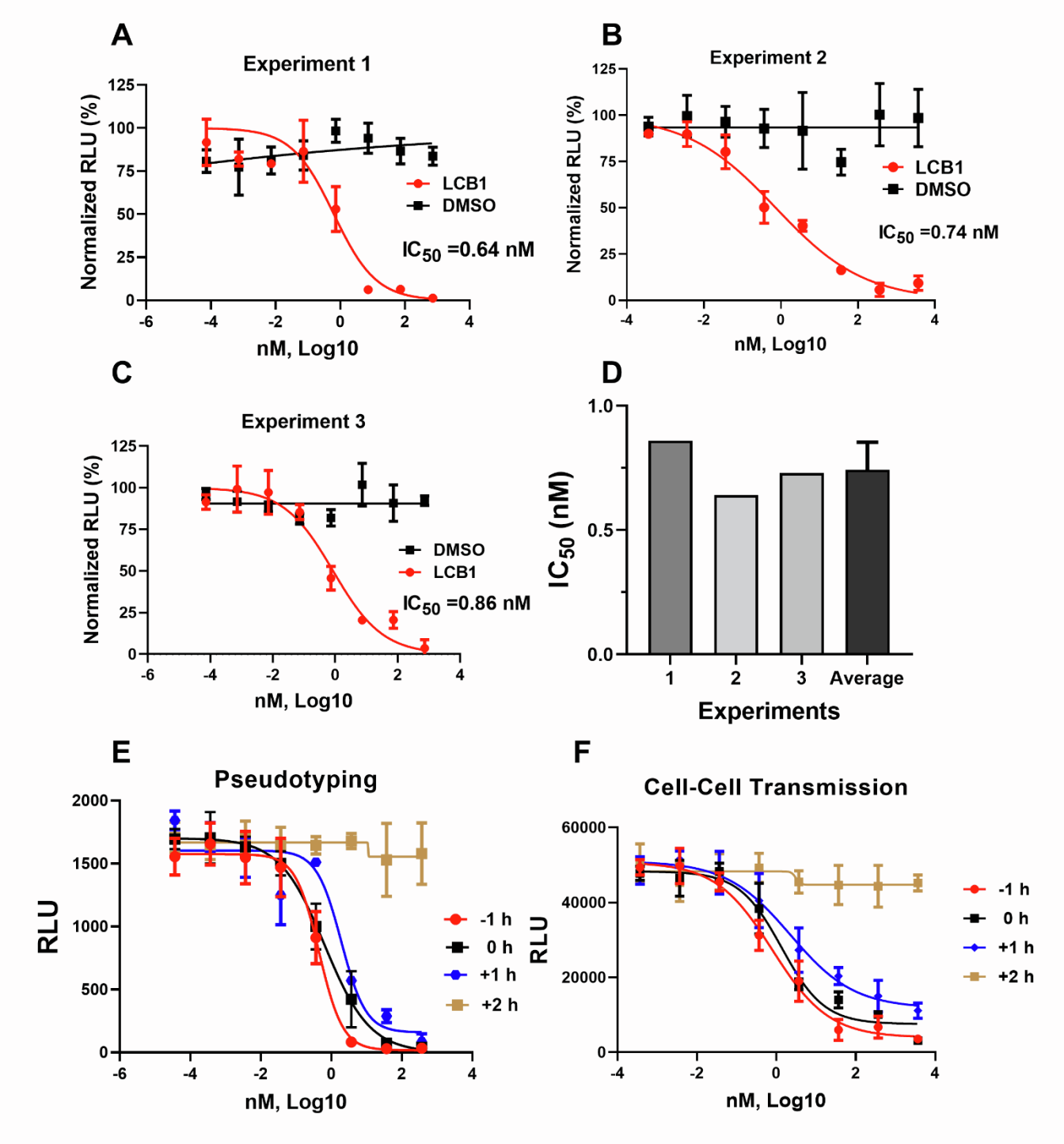

Figure S3. Effect of tetherin on virus infection. Related to Figure 6.

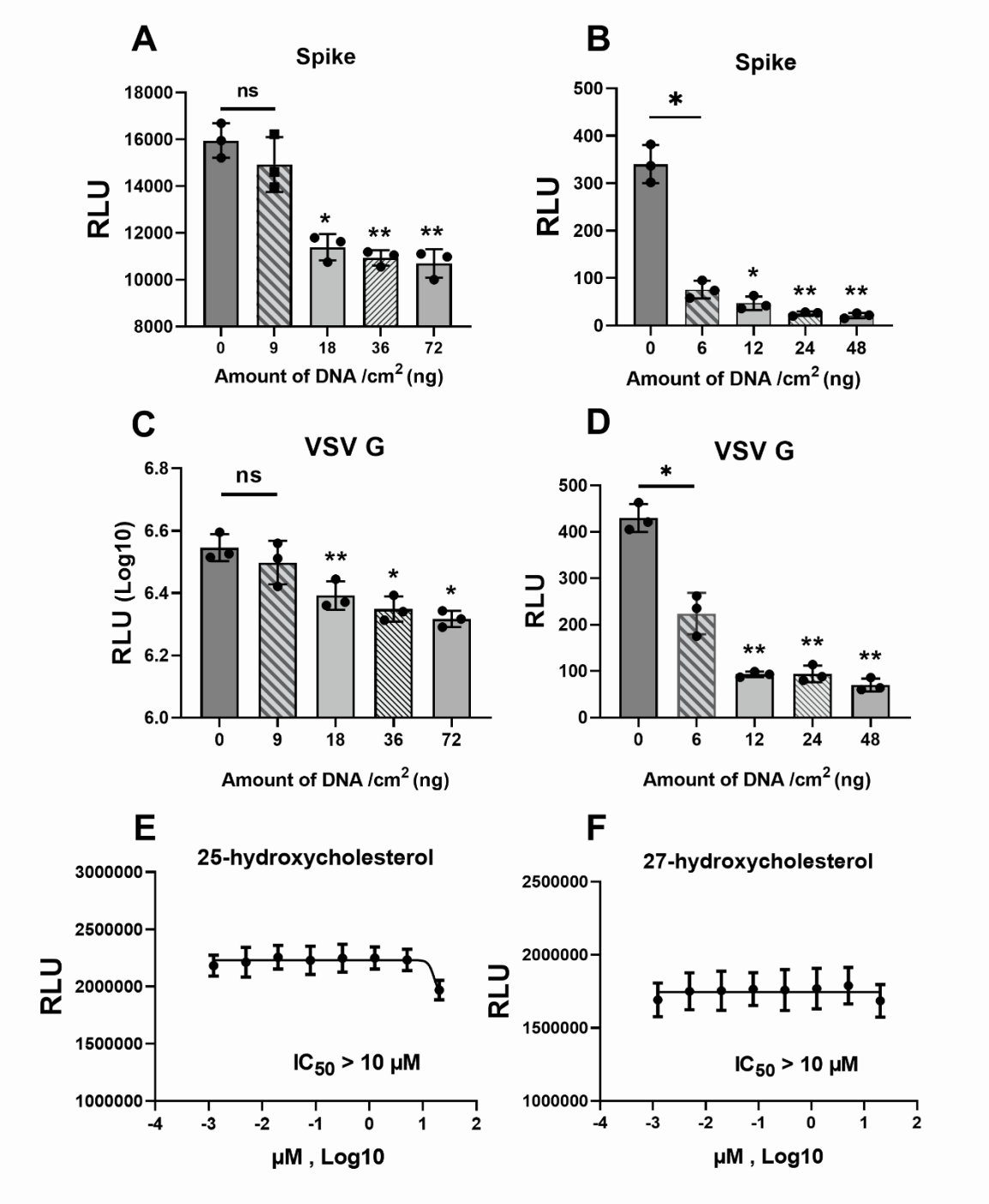

Figure S4. Studies with S variants of concern (VOC). Related to Figures 2, 3 and 4.

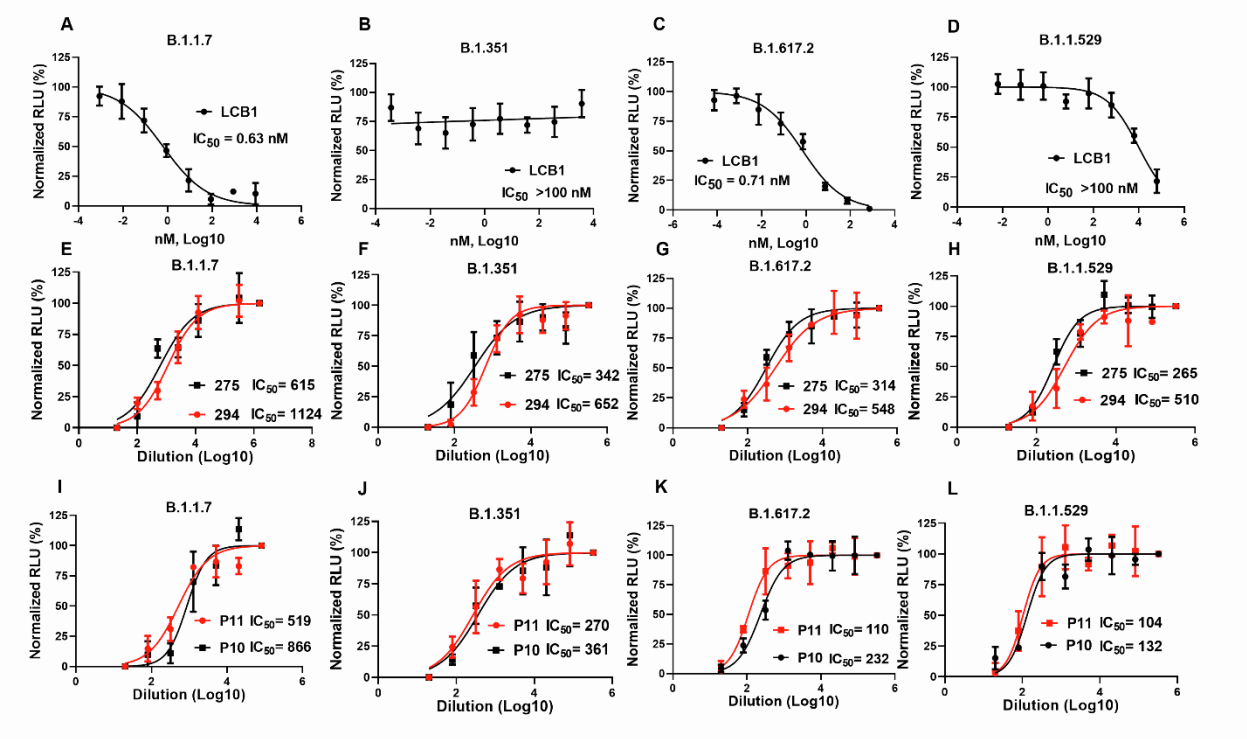

Figure S5. Immunoblotting and PCR of stable cell lines. Related to Figures 5 and 6.

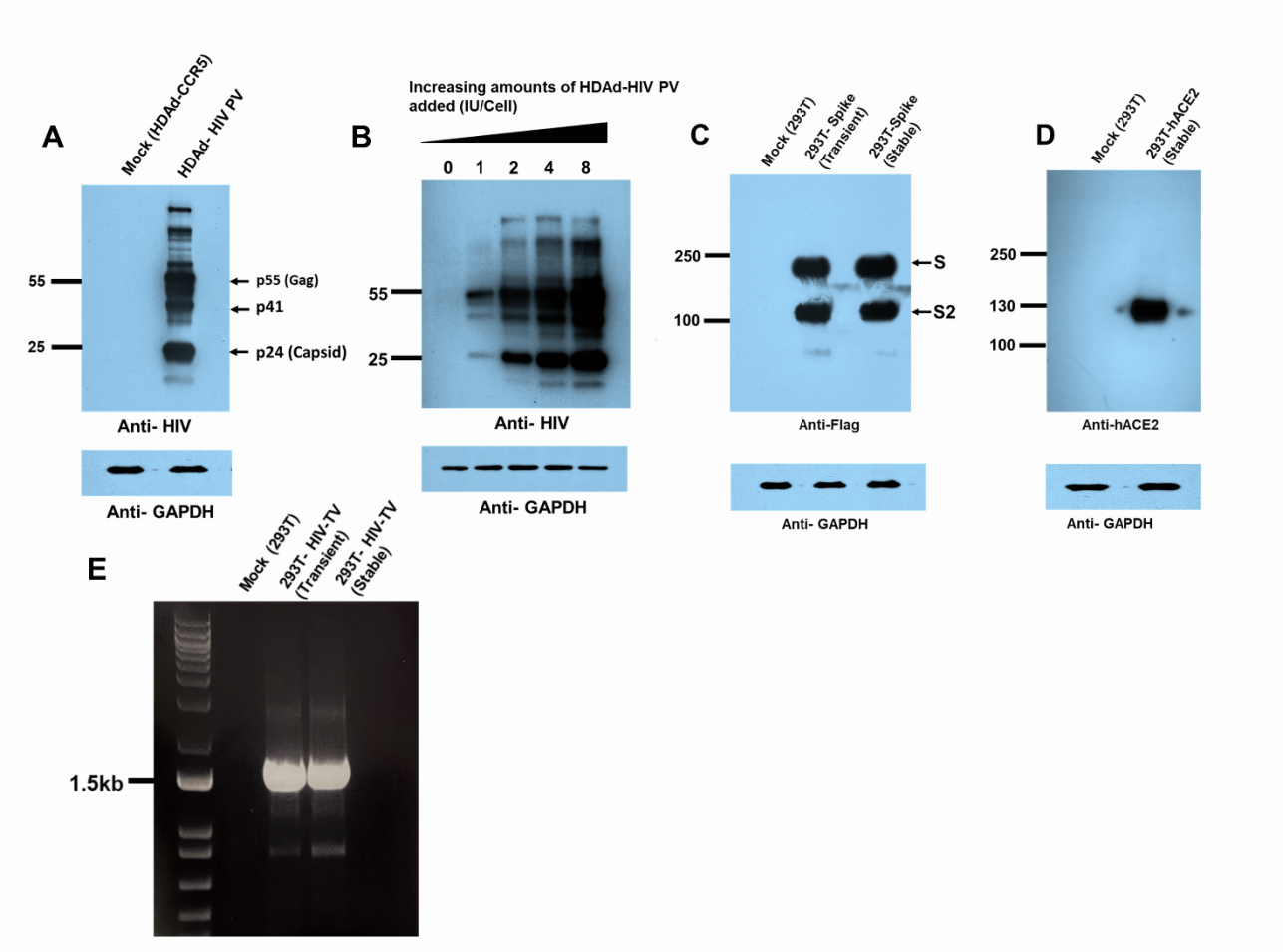

Figure S6. Transduction of stable 293T cells with HDAd-HIV-PV. Related to Figures 5 and 6.

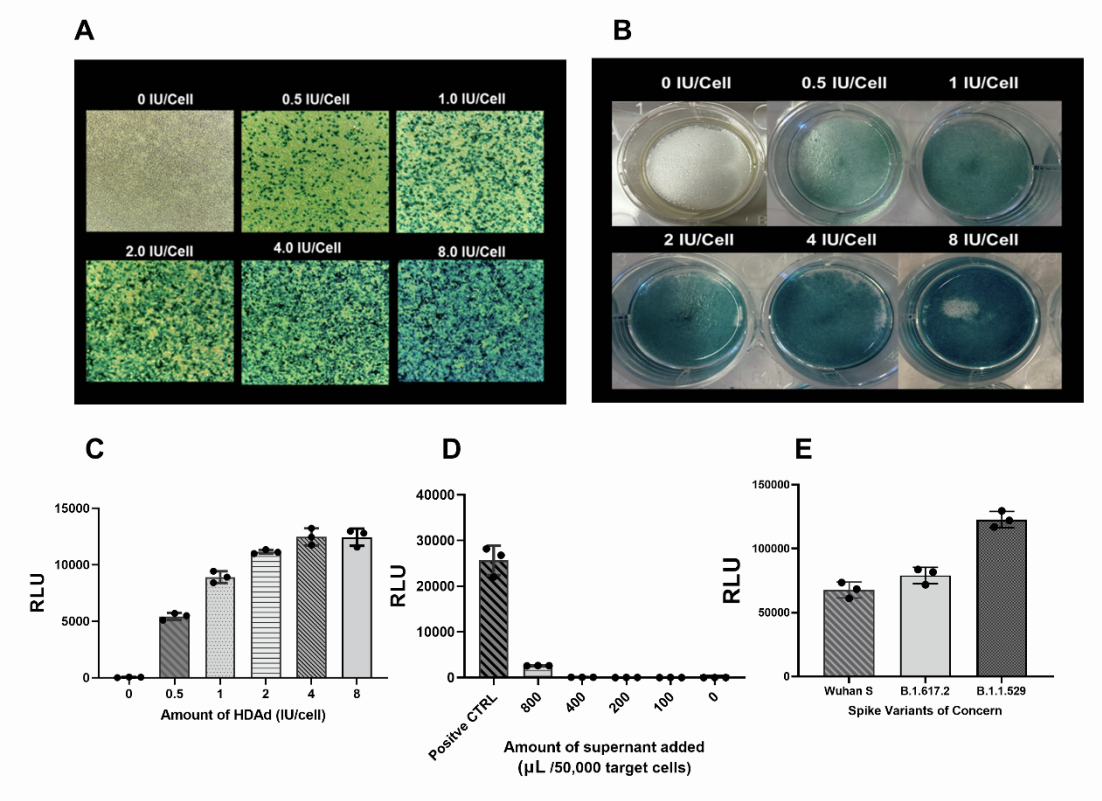

SUPPLEMENTAL TABLES WITH TITLES

Table S1.

Demographic and relevant clinical information of the subjects from whom COVID-19 convalescent sera samples were collected. Related to Figure 2.

Subject ID	Date of sample collection (after symptom onset)	Age	Sex	Race	BMI[a]	Co-morbidities				Severity of disease		Outcome
						Chronic heart disease?	Chronic lung disease?	High blood pressure	Other co-morbid conditions	moderate	severe	
262	21	50	M	hispanic	42			+	diabetes		Intubated[d]	deceased post 1 month
264	7	73	M	black	30			+		Floor[c]		D/C[e] post 1 month
268	8	40	M	asian	29					Floor[c]		D/C[e] at 1 week
271	10	95	F	white	27			+	GERD[j], hypothyroidism	Floor[c]		Deceased post 1 month
272	4	76	M	white	34			+	diabetes	Floor[c]		D/C[e] after 2 days
273	3	66	F	black	37	Afib[f], CHF[b]	COPD[i]	+			Intubated[d]	D/C after 1 month
275	11	86	M	hispanic	25				Diabetes, Alzheimer's dementia	Floor[c]		D/C[e] after 1 week
292	5	69	M	black	27			+		Floor[c]		D/C[e] after 1 week
294	12	65	M	white	46		COPD[i]	+	Diabetes, Hx PE[k]		Intubated[d]	D/C[e] after 2 months
304	16	59	M	Black	16				Hx pancreatitis, alcohol use disorder		Intubated[d]	D/C[e] after 3 weeks

332	8	94	F	black	36	CHF[b]	COPD[i], OSA[g]	+	Breast cancer, GERD[j]		Bipap[h]	Deceased after 6 days

Footnotes:

[a]BMI denotes body mass index

[b]CHF denotes congestive heart failure

[c]Floor denotes subject remained on a regular in-patient unit

[d]Intubated denotes subject was endotracheally intubated in the intensive care unit

[e]D/C denotes discharge from the hospital

[f]Afib denotes atrial fibrillation

[g]OSA denotes obstructive sleep apnea

[h]BIPAP denotes subject required Bilevel Positive Airway Pressure required but not endoctracheal intubation

[i]COPD denotes chronic obstructive pulmonary disease

[j]GERD denotes Gastroesophageal reflux disease

[k]PE denotes pulmonary embolism

Table S2.

Demographic and relevant clinical information of the subjects from whom post-vaccine sera samples were collected. Related to Figures 3 & 5.

Subject ID*	Age	Sex	Race/Ethnicity	BMI[a]	Co-morbidities		
					Chronic heart disease?	Chronic lung disease?	Other co-morbid conditions
P01	65	F	white	27.4	CAD[b]	COPD[c]	
P02	63	M	white	23.3			Hypertension
P03	57	F	white	34.1			Diabetes
P04	56	F	white	26.5			
P05	63	M	white	29.5			
P06	56	F	white	29.2			
P07	38	F	white	27.4			
P08	46	M	white	28.1			
P09	31	F	white-hispanic	23.4			
P10	55	F	white-hispanic	32.1			
P11	40	F	Asian	19.3			

Footnotes:

[a]BMI denotes body mass index

[b]CAD denotes coronary artery disease

[c]COPD denotes chronic obstructive pulmonary disease

*All subjected received the Pfizer vaccine one month prior to blood draw